



Universidade de Aveiro Departamento de Electrónica,
2009 Telecomunicações e Informática

Pedro Miguel Campos **Opportunities of Optical Monitoring Systems using**
de Figueiredo Coelho **XPM effects**

Oportunidades de Monitoria Óptica por recurso a
XPM



Universidade de Aveiro Departamento de Electrónica,
2009 Telecomunicações e Informática

**Pedro Miguel Campos
de Figueiredo Coelho** **Opportunities of Optical Monitoring Systems using
XPM effects**

**Oportunidades de Monitoria Óptica por recurso a
XPM**

Dissertação apresentada à Universidade de Aveiro para cumprimento dos requisitos necessários à obtenção do grau de Mestre em Engenharia Electrónica e Telecomunicações, realizada sob a orientação científica do Dr. António Teixeira do Departamento de Electrónica, Telecomunicações e Informática e do Instituto de Telecomunicações da Universidade de Aveiro.

o júri / the jury

presidente / president

Prof. Dr. José Rodrigues Ferreira da Rocha

Professor Catedrático do Departamento de Electrónica, Telecomunicações e Informática da Universidade de Aveiro

vogais / examiners committee

Prof. Dr. Henrique Manuel de Castro Faria Salgado

Professor Associado do Departamento de Engenharia Electrotécnica e de Computadores da Faculdade de Engenharia da Universidade do Porto

Prof. Dr. António Luís Jesus Teixeira

Professor Associado do Departamento de Electrónica, Telecomunicações e Informática da Universidade de Aveiro (Orientador)

palavras-chave

Sistemas de monitorização óptica, efeitos não lineares, modulação cruzada de fase, mistura de quatro ondas.

resumo

Neste trabalho é apresentado um estudo teórico sobre alguns dos efeitos não lineares que ocorrem nas fibras que suportam as redes ópticas, com especial incidência sobre a modulação cruzada de fase (XPM). Com o objectivo de usar estes mesmos efeitos para monitorizar essas mesmas redes, é também feita uma introdução sobre alguns dos sistemas de monitorização óptica existentes.

Uma técnica de monitoria em redes ópticas com base nos efeitos de XPM é apresentada e estudada. A metodologia assenta na caracterização dos efeitos sofridos por um canal de teste (variância de fase e amplitude) na presença de várias condições de rede. Esta análise confirma que os efeitos da XPM variam com a alteração de alguns parâmetros importantes do sistema, sendo por isso um bom mecanismo de caracterização.

keywords

Optical monitoring systems, nonlinear effects, cross-phase modulation, four-wave mixing.

abstract

This work presents a theoretical study about some of the nonlinear effects that occur in the fibers that support the optical networks. Particular attention will be given to cross-phase modulation (XPM). In order to use these effects to monitor these networks, introductions to some of the existing monitoring systems are also presented.

One monitoring technique in optical networks based on XPM effects is presented and studied. The methodology rests on the characterization of the effects suffered by a probe channel (phase and intensity variance), under several network conditions. This analysis confirms that the XPM effects depend on some of the important system parameters, thus being a good characterization mechanism.

Table of Contents

Table of Contents	i
List of Acronyms	iii
List of Figures & Tables	vii
Chapter 1. Introduction	- 1 -
1.1. Motivation	- 1 -
1.2. Structure and Objectives	- 3 -
1.3. Contributions	- 4 -
Chapter 2. Theory	- 5 -
2.1. Introduction	- 5 -
2.2. Group-Velocity Dispersion.....	- 6 -
2.3. Nonlinear Effects	- 8 -
2.3.1. Nonlinear phase modulation	- 9 -
2.3.1.1. Self-Phase Modulation.....	- 10 -
2.3.1.2. Cross-Phase Modulation	- 12 -
2.3.1.3. Four-Wave Mixing.....	- 16 -
2.3.2. Stimulated light scattering	- 17 -
2.3.2.1. Stimulated Raman Scattering	- 17 -
2.3.2.2. Stimulated Brillouin Scattering	- 18 -
2.4. Modulation Formats	- 18 -
2.4.1. Non-Return-To-Zero	- 19 -
2.4.2. Return-To-Zero	- 20 -
2.4.3. Direct Modulation vs. External Modulation.....	- 21 -
2.5. Monitoring.....	- 23 -
2.5.1. Impairments	- 24 -
2.5.2. Monitoring Techniques	- 25 -

Chapter 3. System Setup	- 35 -
3.1. Emitter	- 36 -
3.2. Fiber	- 38 -
3.3. Receiver	- 38 -
3.4. Measurements.....	- 39 -
Chapter 4. Simulation Results	- 41 -
4.1. Fiber Length	- 42 -
4.2. Fiber Dispersion	- 45 -
4.3. Channel Power.....	- 48 -
4.4. Probe Power	- 49 -
4.5. Number of Channels	- 51 -
4.6. Modulation Format	- 53 -
4.7. Channel Spacing.....	- 55 -
4.8. Bit Rate	- 57 -
Chapter 5. Final Conclusions	- 59 -
References	- 63 -

List of Acronyms

AOWC	All-Optical Wavelength Converter
ASE	Amplified Spontaneous Emission
BER	Bit-Error Ratio
CD	Chromatic Dispersion
CW	Continuous Wave
DCF	Dispersion-Compensating Fiber
DFB	Distributed-Feedback Laser
DFF	Dispersion-Flattened Fiber
DGD	Differential Group Delay
DOP	Degree Of Polarization
DSF	Dispersion-Shifted Fiber
DWDM	Dense Wavelength Division Multiplexing
EAM	Electroabsorption Modulator
EOM	Electrooptical Modulator
FCV	Frequency Chirp Variance
FWM	Four-Wave Mixing
GVD	Group-Velocity Dispersion
HN-DSF	Highly Nonlinear Dispersion Shifted Fibers
IM	Intensity Modulation

IV	Intensity Variance
MZI	Mach-Zehnder Interferometer
NRZ	Non-Return-To-Zero
OADM	Optical Add-Drop Multiplexer
OMS	Optical Monitoring System
OPM	Optical Performance Monitor
OSNR	Optical Signal-To-Noise Ratio
OXC	Optical Cross Connect
PM	Phase Modulation
PMD	Polarization-Mode Dispersion
PON	Passive Optical Network
PSK	Phase-Shift Keying
PSP	Principal States of Polarization
RF	Radio Frequency
RIN	Relative Intensity Noise
RZ	Return-To-Zero
SBS	Stimulated Brillouin Scattering
SMF	Single-Mode Fiber
SPM	Self-Phase Modulation
SRS	Stimulated Raman Scattering
TDM	Time Division Multiplexing

TOD	Third-Order Dispersion
VS	Vestigial-Sideband
WDM	Wavelength Division Multiplexing
XPM	Cross-Phase Modulation

List of Figures & Tables

Chapter 1.

Figure 1.1. Increase of BL product through the generations [1].

Chapter 2.

Figure 2.1. Pulse spreading due to GVD and a bit error example on the receiver.

Figure 2.2. Variation of β_2 with wavelength for fused silica [1].

Figure 2.3. Variation of D with wavelength for SMF [1].

Figure 2.4. Temporal variation of SPM-induced phase shift and frequency chirp.

Figure 2.5. Asymmetric spectral broadening of two copropagating pulses [1].

Figure 2.6. Asymmetric temporal changes on shapes (upper row) and spectra (lower row) of probe and pump Gaussian pulses [1].

Figure 2.7. All-optical wavelength converter structure [6].

Figure 2.8. XPM-induced switching based on a Mach-Zehnder interferometer (MZI).

Figure 2.9. Frequencies generated by FWM.

Figure 2.10. Raman scattering process.

Figure 2.11. NRZ optical spectrum (left) and waveform (right).

Figure 2.12. RZ optical spectrum (left) and waveform (right).

Figure 2.13. Eye diagram for NRZ (left) and RZ (right).

Figure 2.14. Direct modulation (top) vs. External modulation (bottom).

Figure 2.15. Electrooptical modulator.

Figure 2.16. Limitations of OSNR monitoring technique in WDM network (top left), dense WDM network (top right), meshed WDM network (bottom left) and meshed dense WDM network (bottom right) [6].

Figure 2.17. In-band OSNR system by Rasztovits-Wiech, 1998 [6].

Figure 2.18. Vestigial-sideband technique [6].

Figure 2.19. PMD monitoring: frequency sweep over the pulse spectrum (left) and S-parameters (right) [16].

Figure 2.20. Histograms based on electrical sampling (top) and based on optical sampling (bottom) [6].

Figure 2.21. Waveform and power distribution of signal without ASE noise (top) and with ASE noise (bottom) [29].

Chapter 3.

Figure 3.1. System Setup.

Figure 3.2. Intensity and frequency chirp waveforms before (left) and after (right) the propagation.

Table 3.1. Channels parameters.

Table 3.2. Probe parameters.

Table 3.3. Fiber parameters.

Chapter 4.

Figure 4.1. Frequency chirp variance vs. fiber length for different fiber dispersions.

Figure 4.2. Frequency chirp variance vs. fiber length for different number of channels.

Figure 4.3. Intensity variance vs. fiber dispersions for different fiber lengths.

Figure 4.4. Intensity variance vs. fiber length for different fiber dispersions.

Figure 4.5. Intensity variance vs. fiber length for 6 ps/(nm.km) (top) and zoom at the region of the highest value of intensity (bottom).

Figure 4.6. Intensity variance vs. fiber length for 11 ps/(nm.km) (top) and zoom at the region of the highest value of intensity (bottom).

Figure 4.7. Frequency chirp variance vs. number of channels for different channel power.

Figure 4.8. Intensity variance vs. number of channels for different channel power.

Figure 4.9. Frequency chirp variance vs. number of channels for different probe power.

Figure 4.10. Intensity variance vs. number of channels for different probe power.

Figure 4.11. Frequency chirp variance vs. number of channels for different fiber length.

Figure 4.12. Frequency chirp variance vs. number of channels for different fiber dispersion.

Figure 4.13. Intensity variance vs. number of channels for different modulation formats.

Figure 4.14. Frequency chirp variance vs. number of channels for different modulation formats.

Figure 4.15. Intensity variance vs. number of channels for different channel spacing.

Figure 4.16. Frequency chirp variance vs. number of channels for different channel spacing.

Figure 4.17. Frequency chirp variance vs. number of channels for different bit rate.

Figure 4.18. Intensity variance vs. number of channels for different bit rate.

Chapter 5.

Table 5.1. Summary of the monitoring opportunities.

Table 5.2. Important notes regarding some parameters.

Chapter 1. Introduction

1.1. Motivation

Fiber-optic communication has rapidly developed and the new technology aims to offer more bandwidth to as many users as possible over long distances. Since the First Generation of lightwave systems, in the late seventies, the bit rate-distance product, BL (B is the bit rate and L is the repeater spacing), doubles every year (Figure 1.1). Each generation issues had motivated some changes that were needed to improve the performance of the systems. The First Generation systems operated near $0,8 \mu\text{m}$, used GaAs semiconductor lasers and achieved bit rates of 45 Mb/s using repeaters spaced up to 10 km. Since then, from the use of larger repeater spacing (Second Generation), through the design of dispersion-shifted fibers (DSFs – to have minimum dispersion near $1,55 \mu\text{m}$) or the development of lasers oscillating in a single

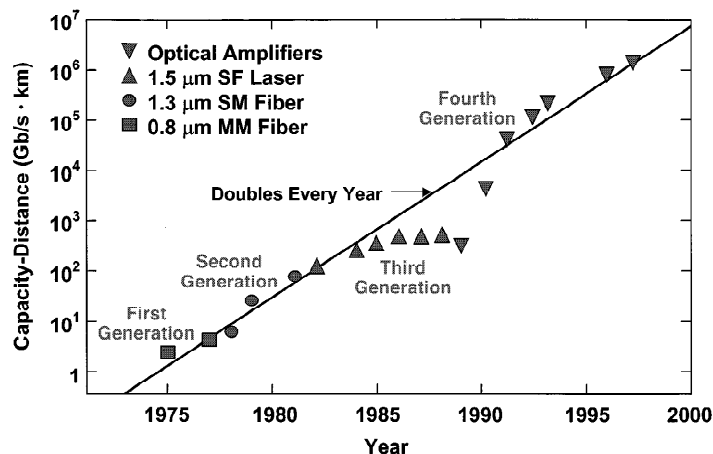


Figure 1.1. Increase of BL product through the generations [1].

longitudinal mode (Third Generation), until the use of optical amplification (so the repeater spacing could be increased) and the advent of the wavelength division multiplexing (WDM) technique (Fourth Generation), many improvements were incorporated to get to the point where technology stands now. However, the potential of fiber-optic systems and the constant demand for more capacity leads the Fifth Generation to focus its work on transmitting even more channels through WDM by expanding the conventional wavelength window (known as the C band and covers 1,53 – 1,57 μm range) on long- and short-wavelength sides (L and S bands, respectively). As Raman amplification can be used in all three wavelength bands and once *dry fiber* was developed (a fiber where the losses are small over wavelength range 1,30 – 1,65 μm, with no H₂O absorption peak), thousands of WDM channels can be transmitted in the newer lightwave systems. Besides offering systems with even higher capacity, the Fifth Generation also intends to increase the bit rate of each channel within the WDM comb. Still, higher bit rates require extreme control of fiber dispersion because nonlinear impairments like self-phase modulation (SPM), cross-phase modulation (XPM) or four-wave mixing (FWM) can greatly degrade system performance. Optical solitons proved to be a good solution as they preserve pulse shape during propagation in a lossless fiber by counteracting the effect of dispersion through the fiber nonlinearity.

Lately, one of the primary motivations of network operators is to reduce the overall cost inherent to the implementation and maintenance of this kind of systems.

As so, the importance of optical monitoring systems (OMS) in next generation networks has highly increased. The success of OMS can avoid unnecessary expenses and its usage is commonly associated with compensating techniques which are, in optimum conditions, controlled by the OMS. The original OMS purpose was to supervise the network and find the location where the faults occurred in order that the maintenance teams could solve the problem. Still, new networks are dynamic and can be constantly changed, which makes the OMS task difficult. So, the ambition is to develop monitoring techniques capable of supporting those changes and create compensating systems that can solve the existing problems. Despite the fact that several techniques have already been developed, there is still a lack of references of monitoring systems that can handle complex scenarios. Since nonlinear impairments become even more important, this thesis intends to give a contribution on OMS by using one of the main sources of signal degradation in WDM systems, the XPM, to enhance supervision of optical networks.

1.2. Structure and Objectives

Although the main focus of this work is on XPM, other important impairments are present in WDM systems. As such, Chapter 2 contains a theoretical analysis of the most important nonlinear effects of fiber-optic communication systems, as well as it explains how group-velocity dispersion (GVD) can have great importance when combined with nonlinearities. Furthermore, several applications of the nonlinear effects such as wavelength converters, among other, are presented. Chapter 2 also shows the main differences between the two most common modulation formats, non-return-to-zero (NRZ) and return-to-zero (RZ), each one's advantages and disadvantages, and a comparison between direct and external modulation. Finally, Chapter 2 is also used to introduce some of the existing monitoring techniques. In Chapter 3, it is presented the system setup used in this work, along with the range of

values of the different parameters that were tested during simulations with software VPI. Simulation results are shown and interpreted in Chapter 4. Lastly, the final conclusions taken from this work are presented in Chapter 5.

1.3. Contributions

In the author's opinion, the main contributions of this work may be summarized as follows:

- Understanding the main nonlinear effects present in a Wavelength Division Multiplexing system, their possible impact in a network, and some of their applications.
- State of the art of the Optical Monitoring Systems.
- Exhaustive study of a technique based in a pump-probe configuration. Probe alterations due to Cross-Phase Modulation are analyzed by measuring its intensity variance and frequency chirp variance.
- Possible applications of the proposed monitoring method.

Besides this final work, a paper was done and accepted by *The 10th International Conference on Telecommunications* (ConTEL 2009 in Zagreb, Croatia):

- P.M. Coelho, J.D. Reis, B. Neto, P.S. André and A. Teixeira, "*Monitoring of Fiber Nonlinearities in WDM Based Passive Optical Networks*", June, 2009.

Chapter 2. Theory

2.1. Introduction

In Chapter 1, we have mentioned that the use of optical fiber based transmission technology has increased once it can provide systems with huge capacities. Next generation networks will aim to offer even higher bandwidth to as many users as possible, covering as much distance as they can. However, to develop networks capable of matching those challenges, engineers have to deal with several limitations inherent in optical fiber transmission systems. Group-velocity dispersion (GVD), polarization-mode dispersion (PMD), and nonlinear effects such as self-phase modulation (SPM), cross-phase modulation (XPM) and four-wave mixing (FWM) are some of the impairments suffered by the signals that can seriously degrade network performance and, therefore, need to be carefully supervised and controlled.

Furthermore, the monitoring of the impairments may and should be used in order to enable compensation and provide flexibility to the network to be able to adapt to the worst conditions.

The main focus of this work is to provide a comprehensive set of guidelines to understand how XPM can be used as a vehicle to enhance supervision of optical networks. Still, it is also important to describe other important impairments to understand how they can be related. This is discussed in Section 2.2. Moreover, some applications of those impairments will be addressed as well. As impairments can depend on modulation chosen to transmit the information, Section 2.3 is devoted to the main characteristics of non-return-to-zero (NRZ) and return-to-zero (RZ) modulation formats and the difference between direct and external modulation. The last section of this chapter, 2.4, is directed to monitoring and the existing techniques in the field.

2.2. Group-Velocity Dispersion

In a single-mode fiber (SMF), different spectral components of a pulse travel at different group velocities, leading to a pulse broadening. This phenomenon is known as GVD and can play a critical role in transmission and, if not properly compensated, can lead to bit errors (Figure 2.1).

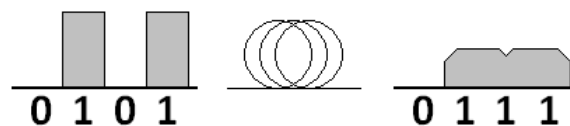


Figure 2.1. Pulse spreading due to GVD and a bit error example on the receiver.

GVD is, usually, represented by its parameter β_2 and varies with wavelength λ for fused silica fibers, as shown in Figure 2.2. Although it may look like β_2 fade near $1,27 \mu\text{m}$ (called zero-dispersion wavelength, λ_D) it is not completely true as pulse

propagation near this wavelength requires the inclusion of third-order-dispersion (TOD) parameter, β_3 , but it is only necessary when wavelength approaches λ_D within a few nanometers.

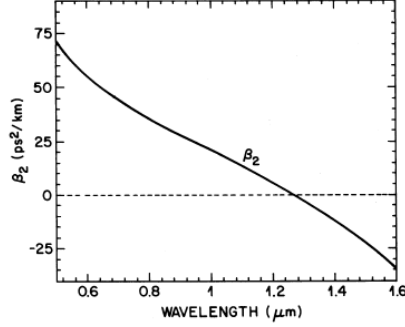


Figure 2.2. Variation of β_2 with wavelength for fused silica [1].

Figure 2.2 is representative of fused silica. Actual fibers may have small quantities of dopants and, besides, because of dielectric waveguiding, the effective mode index is slightly lower than the material index $n(\omega)$ of the core, reduction itself being ω dependent [1]. These differences result in a slight shift of λ_D to near 1,31 μm . Dispersion parameter, D , is normally used instead of β_2 . Figure 2.3 shows the variation of D with wavelength for a SMF. Furthermore, dispersion parameter is related to β_2 by the relation shown in Equation (2.1) [1]

$$D = \frac{d\beta_1}{d\lambda} = -\frac{2\pi c}{\lambda^2} \beta_2 \approx \frac{\lambda}{c} \frac{d^2 n}{d\lambda^2} \quad (2.1)$$

The waveguide contribution depends on fiber parameters, such as core radius and core-cladding index difference, which can be used to shift λ_D to the region where fiber loss is minimum. That dependence gave rise to the development of fibers in which GVD is shifted (e.g. dispersion-shifted fibers (DSFs) and dispersion-compensating fibers (DCFs)) and others where low dispersion can cover a relatively large wavelength range (e.g. dispersion-flattened fibers (DFFs)).

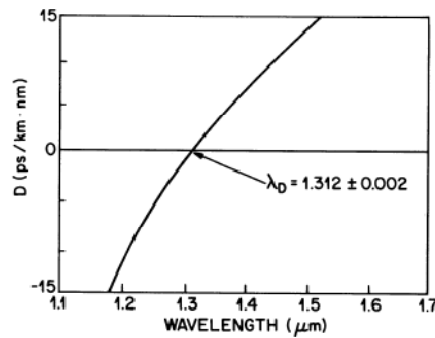


Figure 2.3. Variation of D with wavelength for SMF [1].

2.3. Nonlinear Effects

Before presenting the nonlinear effects that are most relevant for fiber-optic communications, it is essential to know the definition of some important fiber parameters such as effective core area (A_{eff}) and effective length (L_{eff}). A_{eff} is the core area if considering a uniform distribution of the optical intensity inside and zero when out of it. L_{eff} is the fiber length assuming that the power is constant along the considered distance. It can be given by (2.2) [2]

$$L_{eff} = \frac{1}{\alpha} (1 - e^{-\alpha L}) \quad (2.2)$$

As previously said, GVD is the pulse spreading that occurs within a single mode because the different frequency components of the pulse travel at different velocities. When $\beta_2 > 0$ (known as normal dispersion regime) the optical high-frequency components of an optical pulse travel slower, while for $\beta_2 < 0$ (known as anomalous dispersion regime) the optical low-frequency components travel slower.

Since silica presents a small nonlinear index (about $2,6 \times 10^{-20} \text{ m}^2/\text{W}$, depending on dopants used inside de core) this can lead us to think that their nonlinearities would be negligible. However, fibers' small core size and usual long lengths can enhance strongly the nonlinear effects in a way that the information can be degraded.

The response of any dielectric to light becomes nonlinear for intense electromagnetic fields. Optical fibers are no exception and the optical response of the material can be represented by an expansion of the polarization field vector (2.3) [1]

$$P = \varepsilon_0 (\chi^{(1)} \cdot E + \chi^{(2)} : EE + \chi^{(3)} : EEE + \dots) \quad (2.3)$$

where ε_0 is the vacuum permittivity and $\chi^{(n)}$ is the n^{th} order susceptibility to optical frequencies. The effects of the first order susceptibility, $\chi^{(1)}$, include refractive index, n , and the attenuation coefficient, α , and they are the main contribution to P . The second order susceptibility, $\chi^{(2)}$, can be considered zero because of the glasses' optical isotropy. The third order susceptibility, $\chi^{(3)}$, effects can be divided into two classes: elastic and inelastic.

Elastic when no energy is exchanged between the electromagnetic field and the dielectric medium. In this case, the nonlinear effects occur because the refractive index (in a silica fiber) depends on intensity changes in the signal. This can result in phase modulation (e.g. SPM and XPM), in the generation of new frequencies (e.g. FWM) or other.

The stimulated inelastic scattering processes arise from the transfer of part of optical field energy to the nonlinear medium. A photon is scattered to a lower energy photon resulting in a phonon which is the energy difference between both photons (e.g. optical phonons in Raman scattering and acoustic phonons in Brillouin scattering).

2.3.1. Nonlinear phase modulation

It was previously stated that the refractive index n depends on optical intensity I . That dependence is given by (2.4) [1]

$$n = n_0 + n_2 I = n_0 + n_2 \frac{P}{A_{eff}} \quad (2.4)$$

where n_0 is the linear refractive index of the material, n_2 is the nonlinear index coefficient, P is the optical power and A_{eff} is the effective area. The relation between n_2 and $\chi^{(3)}$ is given by (2.5) [1]

$$n_2 = \frac{3}{8n_0} Re(\chi^{(3)}) \quad (2.5)$$

The intensity dependence of the refractive index results in nonlinear effects such as SPM and XPM.

2.3.1.1. Self-Phase Modulation

The dependence of the refractive index on optical intensity produces a nonlinear phase shift, ϕ_{NL} , while a signal propagates through an optical fiber given by Equation (2.6) [3]

$$\phi_{NL} = \gamma P_0 L_{eff} \quad (2.6)$$

where [3]

$$\gamma = \frac{2\pi n_2}{A_{eff}\lambda} \quad (2.7)$$

and P_0 is the peak input power.

SPM induces spectral broadening, since P_0 is time dependent and, consequently, ϕ_{NL} will also vary with time as its nonlinear phase depends on field amplitude. Once the phase varies temporally, the instantaneous optical frequency will also differ across the pulse from its central value, which means that frequency is also time dependent. The frequency time dependence is commonly known as frequency chirp and it leads to a spectral broadening, new frequency components are generated through fiber propagation [1] (Figure 2.4).

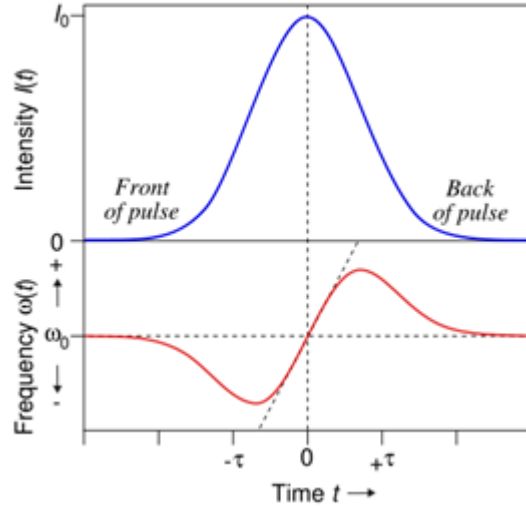


Figure 2.4. Temporal variation of SPM-induced phase shift and frequency chirp.

Spectral broadening magnitude is given by the highest value of frequency chirp which depends on pulse shape. Further, the broadening increases linearly with peak power P_0 because φ_{NL} depends on intensity (Equation (2.6)) and frequency chirp depends on φ_{NL} (Equation (2.8) [1]).

$$\delta\omega(T) = \frac{\delta\varphi_{NL}}{\delta T} \quad (2.8)$$

Along with spectral broadening, SPM also implies an oscillatory structure that is a consequence of time dependence of the frequency chirp, as referred in Figure 2.4. In general, the same chirp occurs at two values of T , showing that the pulse has the same instantaneous frequency at two distinct points. These two points represent two waves of the same frequency but different phases that can interfere constructively or destructively, depending on their relative phase difference. Therefore, the number of peaks depends on φ_{max} and the outermost are the most intense [1].

The combined effects of SPM and GVD can give rise to new features as optical solitons (when considering the anomalous-dispersive regime) or pulse compression (the case of normal-dispersion regime). In the latter, a pulse broadens faster than in the absence of SPM once self-phase modulation generates new frequency components, as previously referred. In the former, optical solitons can be used to

maintain a chirp-free pulse because the SPM-induced chirp may nearly cancel the effect of the dispersion-induced chirp as the two have opposite signals [1],[4],[5].

2.3.1.2. Cross-Phase Modulation

XPM is very similar to SPM. The difference is that XPM occurs when two or more optical channels propagate simultaneously through a fiber (instead of only one in SPM) as in a wavelength division multiplexing (WDM) system. The nonlinear phase shift also depends on the power of other channels, so the phase shift for the j^{th} channel can be given by (2.9) [3]

$$\phi_j^{NL} = \gamma L_{eff} (P_j + 2 \sum_{m \neq j} P_m) \quad (2.9)$$

Expression (2.9) shows that XPM (second term in Equation 2.9) occurs together with SPM (first term) and, when the channels optical power is the same, XPM effect is twice stronger than SPM. When one of the beams is stronger than the other (usually the pump is stronger than the signal or some probe), the weakest beam will primarily suffer the effect. Thus, refractive index seen by an optical field in a fiber depends on the square of the intensity of its own field and the other copropagating fields and we can rewrite the nonlinear phase shift expression as shown in Equation (2.10) [1]. Considering only two signals, probe and pump:

$$\phi_i^{NL} = n_2(\omega_i/c)(|E_i|^2 + 2|E_j|^2) \quad (2.10)$$

When the probe is much weaker than the pump, Equation (2.10) shows that the probe influence on the nonlinear phase shift induced by it is negligible and the phase shift is nearly only SPM responsibility.

The main difficulty on estimating the XPM impact is related to pulses from different channels not travelling at the same speed and the XPM nonlinear phase shift

only occur when two or more pulses overlap in time. That means, for widely separated channels the XPM effect can be negligible as the time in which the channels overlap is too short. XPM bandwidth was studied in [6] and is usually hundreds of gigahertz, and can even achieve over 1 THz using highly nonlinear dispersion shifted fibers (HN-DSFs) [6].

Another important feature of XPM is the asymmetric spectral and temporal changes that it brings. Consider two pulses copropagating where $P_2 > P_1$ and assume that $L \ll L_D$ and $L_W < L$ (where L is fiber length, L_D is dispersion length and L_W is walk-off length). L_W can be defined as a measure of the fiber length during which two overlapping pulses separate from each other, as a result of the group-velocity mismatch [1]. It was previously mentioned that the time dependence of the phase result in spectral broadening. Thus, like happened in SPM, the spectrum of each pulse broadens and develops an oscillatory structure. However, with XPM contribution some modifications will rise. A spectral asymmetry will occur in both pulses spectrum and the asymmetry is greater in pulse 2 spectra as it suffered more XPM effects (as shown in Figure 2.5).

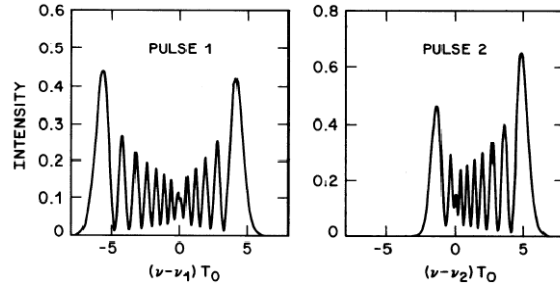


Figure 2.5. Asymmetric spectral broadening of two copropagating unchirped Gaussian pulses [1].

Previous case neglected GVD effects because it was considered $L \ll L_D$. As a result, pulse shapes remained unchanged once all of their components were propagating at the same velocity. If L_D becomes comparable with L or L_W , not only spectral variations occur, but also temporal changes will appear. Consider now a pump-probe configuration ($P_1 \gg P_2$) where pump travels faster than the probe. Once $P_1 \gg P_2$, we can consider that pump pulse is unaffected by the probe pulse and, consequently, suffers the combined effects of SPM and GVD. In contrast, probe pulse

is affected considerably by the pump pulse, so its shape and spectrum are governed by the combined effects of XPM and GVD (SPM can be neglected as discussed in Equation 2.9). As GVD is considered, different parts of the probe will travel at different speeds as a result of XPM-induced chirp. This results in an asymmetric shape in the probe pulse (Figure 2.6).

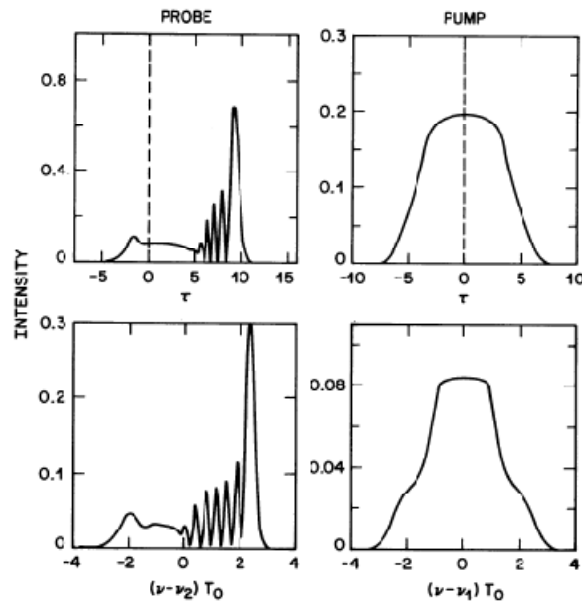


Figure 2.6. Asymmetric temporal changes on shapes (upper row) and spectra (lower row) of probe and pump Gaussian pulses [1].

Although XPM often limits the system performance, in some cases, it can also be beneficial and can be used for several applications in optical communication networks like wavelength conversion, demultiplexing, switching, pulse compression, among others.

Wavelength conversion can be made through FWM, but using XPM makes the process more flexible, which anticipates XPM-based fiber all-optical wavelength converters (AOWC) a bright future at ultra-high bit rates conversion [6]. The conversion is made by transferring the information carried on the intensity of the input signal into a phase modulation of the continuous wave (CW). Then it is needed to convert that phase modulation, PM, imprinted on the CW, into intensity modulation, IM (Figure 2.7).

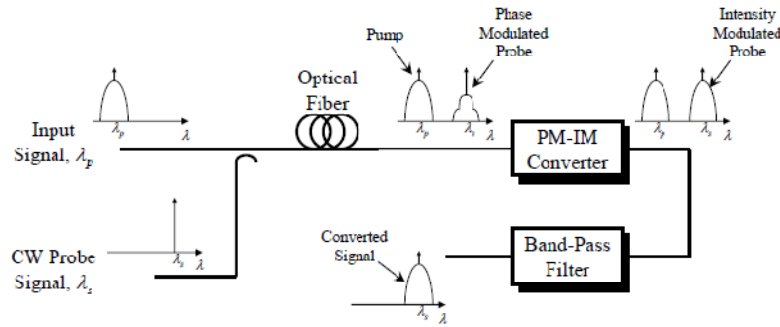


Figure 2.7. All optical-wavelength converter structure [6].

Unlike FWM-based converters that need specific input wavelengths in order to achieve the desired output signals, in XPM-based converters the wavelength of the output does not depend on the wavelength of the input one. The great disadvantage of this technique is the requirement of IM input signals, although it is possible to deal also with PM signals by applying a PM-IM converter before the AOWC.

Another XPM application is optical switching. It can be achieved by a PM-IM interferometer where a weak pulse is divided equally into its two arms and each arm will suffer the same phase shift. By transmitting a pump pulse at a different wavelength in one of the arms, the phase shift will change because of XPM and it will not be equal to the other arm. If the new phase shift is large enough (near π) the output will experience destructive interference and the signal is not transmitted (Figure 2.8).

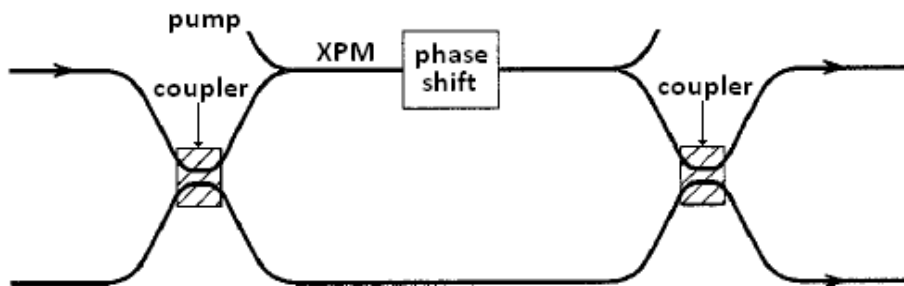


Figure 2.8. XPM-induced switching based on a Mach-Zehnder interferometer (MZI).

This type of applications has great importance in optical communication systems as some of the electric components used in some networks could be replaced with all-optical ones, tending to improve transparency and speed.

2.3.1.3. Four-Wave Mixing

FWM is also originated by $\chi^{(3)}$ but this phenomenon involves not only a modulation of the index but also an energy transfer between the optical waves. In a WDM system, the propagation of two or more channels causes the generation of one or more new frequencies. For example, if we have three carrier frequencies ω_1 , ω_2 and ω_3 propagating simultaneously through an optical fiber, a new frequency ω_4 will be generated and it is related to other frequencies by $\omega_4 = \omega_1 \pm \omega_2 \pm \omega_3$. This procedure is innocuous up to the point when the new frequency falls in the transmission window, near one channel, causing crosstalk. Figure 2.9 shows the FWM effect for two signal frequencies.

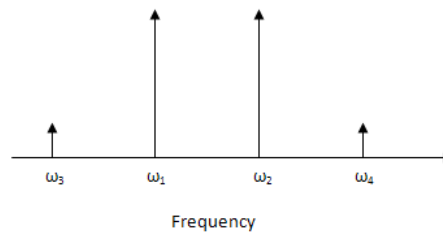


Figure 2.9. Frequencies generated by FWM.

where $\omega_3 = 2\omega_1 - \omega_2$ and $\omega_4 = 2\omega_2 - \omega_1$. It can be seen that two copropagating waves generate another two frequencies and, for N wavelengths transmitted through a fiber, the number of new frequencies generated M is [1]

$$M = \frac{N^2}{2} (N - 1) \quad (2.11)$$

When $\beta_2=0$, FWM is completely phase matched and when β_2 and channel spacing are small ($\beta_2 < 1 \text{ ps}^2/\text{km}$ and channel spacing less than 100 GHz) the process can still occur and the power transfer is made from each channel to its nearest ones. It leads to power loss and interchannel crosstalk and, consequently, the degradation of the system performance [1],[2],[7]. The common solution to this problem is controlling the dispersion, maintaining GVD locally high but low on average.

Despite being harmful by inducing crosstalk in WDM systems (even though FWM can be avoided using different spacing between channels or utilizing fibers with such GVD that FWM is not phase matched), FWM can also be useful and there are some applications where FWM has great importance, as wavelength conversion and sampling (among others, like parametric amplification, optical regeneration, etc.).

2.3.2. Stimulated light scattering

It was already been said that in stimulated inelastic scattering there is a transfer of part of the optical field to the nonlinear medium. Two of these effects are known as stimulated Raman scattering (SRS) and stimulated Brillouin scattering (SBS).

2.3.2.1. Stimulated Raman Scattering

Raman scattering occurs when a pump photon, ω_p , excites a molecule to a virtual level. As the molecule decays to a lower energy level, a photon ω_s is emitted. The difference in energy between the two photons is absorbed by the nonlinear medium as molecular vibrations. In the Raman scattering case, the phonons created are optical. The process is shown in Figure 2.10:

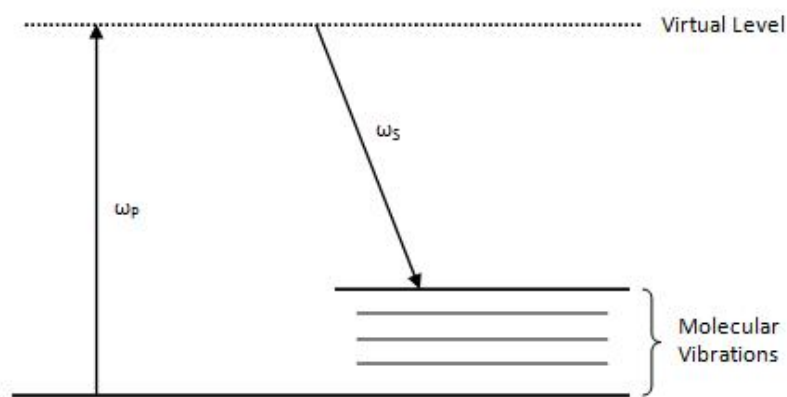


Figure 2.10. Raman scattering process.

The wavelength difference between the two photons (pump and signal) is known as Stokes shift, $\Omega = \omega_p - \omega_s$, and its maximum value occurs at $\Omega \approx 13,2$ THz. In SRS, the light wave generated is scattered in both directions, forward and backward, although more efficiently in the forward direction. For low energy levels SRS effect is also low and can be negligible. However, when considering higher energy levels, there is a threshold of, approximately, 600 mW, from which SRS becomes a problem [1]. Also, the large gain bandwidth of SRS enables it to couple different channels in a WDM system which can originate crosstalk and cause performance degradation in the network.

2.3.2.2. Stimulated Brillouin Scattering

Brillouin scattering principle is almost the same as Raman. There are three main differences between the two effects. First, in SBS the phonons created are acoustic and, consequently, the Stokes shift is $\Omega \approx 10$ GHz, much lower than in SRS case. Second, the Stokes wave is only backscattered which results in less degradation in the forward propagation when compared to other nonlinear effects. Usually optical amplifiers have one or more isolators so accumulations of the backscattered light are prevented. The third difference is the threshold that is only a few milliwatt. In SBS the gain bandwidth is narrow and much lower than in SRS, which prevents interactions among channels in a WDM system [1].

2.4. Modulation Formats

One target of the present optical communication systems is to extend the number of channels, which is being done by extending to the close wavelength bands

(L-band and S-band). Besides, a parallel path is being followed which bases its evolution in the increase of the line rate per channel (10, 40 and 100 Gb/s and plus are being deployed all over [8]-[10]). However, this task is not so easy to accomplish as the new systems demand new dispersion compensation management (chromatic dispersion, CD, and first order PMD) and the nonlinear effects (like SPM, XPM and FWM) highly degrade the performance. In this study, two of the most common modulation formats were investigated and their characteristics will now be discussed.

2.4.1. Non-Return-To-Zero

NRZ has been the main modulation format and used extensively in fiber-optical communication systems (Figure 2.11) and only nowadays it is being slowly upgraded to new coherent and phase based modulation formats. The primary reason for that to happen is the fact that it is easily generated and its bandwidth is about two times smaller than the return-to-zero format (RZ) [3],[11].

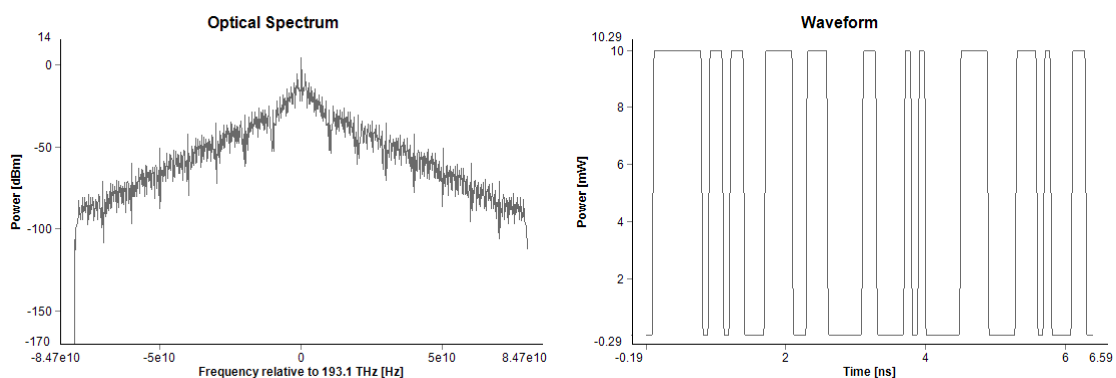


Figure 2.11. NRZ optical spectrum (left) and waveform (right).

The reasons that lead to a decrease in NRZ usage are less resistance to residual chromatic dispersion in an amplified fiber system with dispersion compensation (although NRZ, generally, presents the most compact spectrum compared with the other modulation formats), less tolerance to XPM and FWM in DWDM systems (due to its strong carrier component in the optical spectrum) and less resistance to GVD-SPM

effect, when comparing with RZ [11],[12]. There is also the residual clock recovery component. Nevertheless, NRZ is still applied and, due to its simplicity, it was used in this study.

2.4.2. Return-To-Zero

Alternatively to NRZ, RZ modulation format has been studied since the very end of the last century as its use proved very helpful in the design of new high capacity systems (Figure 2.12). Since RZ is based on a bit commutation to the “0” level, it has, independently of the number of consequent similar symbols, a pattern that allows similar behavior, in power, of the pulses. This fact makes it potentially more tolerant to nonlinearities, since they are more or less affecting all the pulses the same way. When comparing to NRZ it can be seen that the spectrum of RZ is wider because of its narrower pulse width which results in a less spectrum efficiency. A great advantage of RZ is its inhaled clock component that is very useful in receivers.

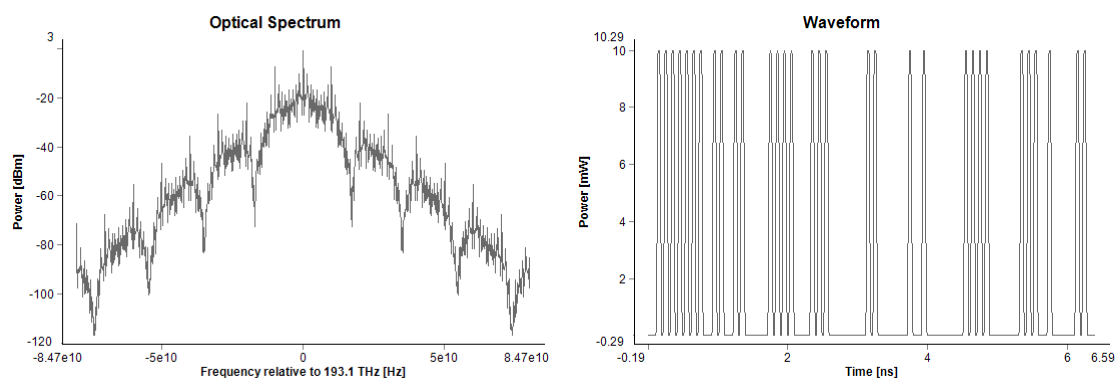


Figure 2.12. RZ optical spectrum (left) and waveform (right).

Not only RZ achieves better performance but also preserves laser durability [11] and has the advantage of being self-synchronized. Despite all RZ advantages, it requires more bandwidth and power than NRZ, becoming for that reason potentially more expensive and spectrally less efficient than NRZ. RZ modulation format is favored in submarine systems (costly transmitters and receivers are used) and NRZ is

commonly employed in terrestrial WDM systems (where cost is a major factor when choosing optical components) [11].

Figure 2.13 shows eye diagrams for both modulation formats.

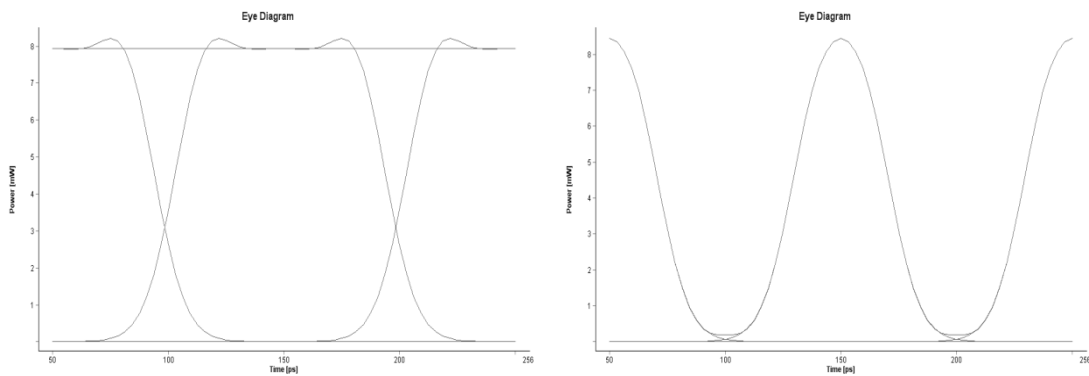


Figure 2.13. Eye diagram for NRZ (left) and RZ (right).

2.4.3. Direct Modulation vs. External Modulation

Modulation is the name given to the process of inscribing information on a light stream and it can be done either directly or externally (Figure 2.14). Direct modulation is done by varying the laser drive current with the information stream to produce a varying optical output power. External modulation demands the use of an external modulator that modifies the steady optical power emitted by the laser.

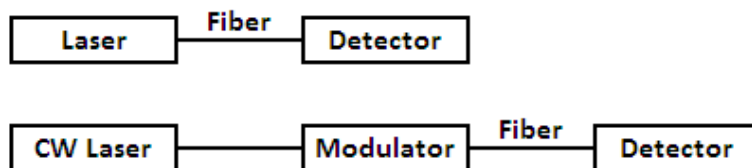


Figure 2.14. Direct modulation (top) vs. External modulation (bottom).

Direct modulation has some advantages like simplicity, compactness and efficient coupling of laser output power to the fiber. However, because turning the drive current on and off produces a widening of the laser linewidth and, in order to minimize undesirable effects, direct modulation is not, normally, a good solution for high-speed systems (higher than 2,5 Gb/s). Those systems, usually, require an external modulator that can be physically integrated in the same package with the light source or in a separate device [13]-[15]. External modulators can be divided in two main types, the electrooptical modulators (EOM) and the electroabsorption modulators (EAM) [3],[16],[17].

EOMs are usually made of lithium niobate (LiNbO_3) and they are separately packaged. This device operation is shown in Figure 2.15 and consists in half splitting the light beam and then sending each half through two separate paths (it can be done using a switch like the one in Figure 2.8). After that, the light signal has its phase changed in one of the paths by one high-speed electric signal. Finally, when both paths meet again at the device output, the two halves of the signal will be recombined either constructively (a bright light is produced and it corresponds to a “1” pulse) or destructively (the two halves cancel each other so no light is produced and it corresponds to a “0” pulse).

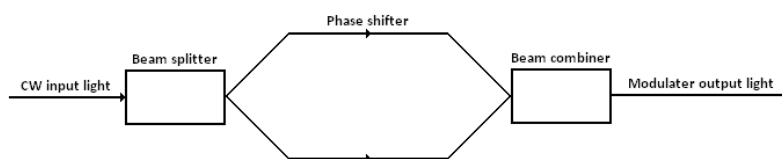


Figure 2.15. Electrooptical modulator.

EAMs are, usually, constructed from indium phosphide (InP) and they can be integrated onto the same substrate as a distributed-feedback laser (DFB) diode chip, reducing drive voltage, power and space requirements when comparing to EOMs. The “0” or “1” pulses are achieved by changing the transmission properties of the material in the light path. That change is caused by an electric signal resulting in a “1” pulse when material is transparent and “0” pulses occur when material is opaque.

In this work, since the simulations were made for bit rates of 2,5 and 10 Gb/s, external modulation is used with a MZI.

2.5. Monitoring

The monitoring of optical networks is becoming even more essential. With the evolution of transmission systems the control of some of the signal properties is very important in order to achieve good performance and avoid any problem that can put it at risk or assure interfacing with other networks at required level. Besides, with adequate monitoring techniques, it is possible not only to prevent issues, but also to compensate any impairment when there is no way to avoid it. That compensation is made through compensation systems that receive the fault localization and reroute the traffic, maintaining the network operating in an optimal manner.

Because there are many signal properties that can and need to be measured, the ideal optical performance monitor (OPM) should do it all. As it looks impossible to achieve that, many OPM are required and its deployments will, obviously, depend on their cost and the benefits that they can bring to the network.

Besides, the new optical networks call for transparent monitoring techniques which are much more expensive as electronic components will be replaced by optical ones. So, the interest in OPMs has grown and it has become a very important feature. However, there are not yet available monitoring techniques as effective as the ones made with electric components. In order to balance this lack in monitoring coverage, tighter engineering rules and more aggressive component specifications are being applied until new and cost-effective OPM are developed and released [18].

2.5.1. Impairments

There are many external parameters capable of harm and damage the normal operation of WDM/TDM-PONs such as physical attacks, temperature variations, vibrations, connection degradation or user's addition and miss-operations. As it is difficult to predict most of these phenomena, robustness and resiliency are becoming even more important features in next generation passive optical networks (PONs) where the number of clients and the distance covered is largely increasing. Thus, new monitoring and compensation strategies must be developed, because there are not many capable of working in this complex scenario, where the demands vary rapidly. Furthermore, high bandwidth connections among hundreds of connected interfaces must be supported.

It is possible to sort the optical impairments in three categories: noise, distortion and timing. The first class relates to random signal fluctuations, which can be signal level dependent; the second one concerns to the modification of the average signal waveform and can be signal level and pattern dependent; timing category refers to fluctuations in the time registration of the bits. Inside these categories there are many effects responsible for the impairments, many of them can occur in more than one category, and can also be divided in component faults or optical transmission impairments.

It is easy to understand that component faults result from components failures, wrong installation or configuration of the equipment and network damage, and these impairments are as many as the number of existing components and network designs.

In transmission impairments many known effects cannot be eliminated and the main objective is to reduce and control the damage that they bring to the network. It can be done through proper design of the network, which has to be able to handle the worst-case impact of any impairment. Some of the existing and most common transmission impairments are amplifier noise, CD, PMD, fiber nonlinearities induced

distortion and crosstalk (SPM, XPM, FWM, SRS, SBS), timing jitter, interference effects, optical filter distortion, linear crosstalk, among others.

Another important resulting problem is the interplay of impairments as there are interactions between them. For example, the impact of XPM is dispersion dependent. So, it is important that any monitoring techniques developed can support network changes like distance and channel configuration, among others, in order not to restrict their usage to non-reconfigurable networks.

Another main issue regarding a good monitoring technique is the impact that it can bring to optical networks maintenance and their troubleshooting procedures. Troubleshooting is usually made by several attempts in different places to discover the exact point where the failure is located. As the number of trials and components tested increase, the cost of this process (related to operator) can grow rapidly. Thus the higher the precision of monitoring system, the smaller the risk of sending repair teams to wrong location and the smaller the recovery time. That is an issue when monitoring systems, which obviously have their cost, but they can save other expenses. The decision of either applying or not (or developing or not) a given technique must be taken considering what benefits it can bring to the network and if those benefits are worth the cost [18].

2.5.2. Monitoring Techniques

The introduction of WDM systems in the beginning of the nineties brought with it the interest in optical monitoring techniques especially when it relates with undersea transmission systems where repair costs tend to be high. But even terrestrial systems began to demand monitoring techniques and the first ones focused on measuring the optical spectrum, although economical methods only appear in the last years of the same decade [18].

One big problem regarding optical monitors, when comparing with electronic alternatives, is the fact that parameters that are monitored have been standardized in the latter. In the former, there is no standard yet and the main reason for this difficulty is that OPM is physical layer monitoring and, therefore, depends on the physical network design. Besides, a single chip is usually enough to implement an electronic performance monitor while good optical performance monitors often require different monitors and components.

From an optical signal there are many measurements that can be performed: average power (per wavelength or aggregate), peak power, pulse or bit shape, eye diagram, intensity or field autocorrelation (including higher order), amplitude power spectrum (radio frequency (RF) spectrum), polarization state, optical spectrum, amplitude histogram (synchronous and asynchronous), Q-factor or bit error rate (BER), polarization mode dispersion (including higher order), chromatic dispersion and phase or optical carrier characteristics. Not only is there a great variety of possible measurements but also, inside each of them, there are even more signal quality parameters (e.g. in-band optical signal-to-noise ratio (OSNR), accumulated CD, bit rate, jitter, etc.) [18].

Because of the difficulty to choose and measure the important parameters for each network, monitoring the optical channels in a WDM system became a good strategy to supervise and control the impairments that are present or can be present in an optical network. The common measurements done in this case are aggregate power, channel power and wavelength and spectral OSNR, and the important parameters monitorized are in-band OSNR, Q-factor (or BER), PMD, accumulated CD, bit rate and jitter.

OPMs are sensitive to the SNR of the optical signals and can be either analog or digital. Although digital techniques make use of high-speed logic to infer the characteristics of the optical signal and have the strongest correlation with BER, they are less effective at isolating the effects of individual impairments. Analog techniques can measure specific characteristics of the waveform both in time domain (e.g. eye diagram, among others) and spectral methods (the most commonly are optical

spectrum and amplitude power spectrum). On the one hand, optical spectral measurements give optical noise information by using highly sensitive optical techniques. On the other hand, amplitude power spectrum provides better estimation of signal quality as it measures the spectrum of the signal that is encoded on the optical carrier (considering intensity modulated formats). By analyzing these aspects it is usually possible to conclude the presence (or not) of an impairment on the signal [18].

Monitoring techniques based on amplitude power spectrum usually make use of spectral tones [18]-[20]. These narrowband signals are superimposed on the data signal and used as monitoring probes. Each tone is at a single and low frequency and they are easily generated. Normally, in pilot tones based techniques, an RF sinusoidal modulation is placed on the optical signal at the transmitter. Different RF frequency tones are assigned to each WDM channel and the average power in these tones will be proportional to the average optical power in the channel. As so, all channels' tones will appear in the RF power spectrum in the same way as they would appear in the optical spectrum. Moreover, the noise between the tones will be proportional to the optical noise (unless cases where ghost tones may appear). The big advantage of these techniques is the encoding on the electrical spectrum (or RF power) of an image of the optical spectrum. Thus, the signal can be monitored without the need to detect baseband data directly and a strong correlation with the transport degradation mechanisms is maintained. [18], [21]. In addition, there is also the possibility of using the tones to measure the accumulation of CD and PMD on a digital signal. However there are also some problems regarding the use of tones. The most important is the occurrence of ghost tones which result from cross-gain modulation in optical amplifiers [18]. These tones are written from one channel to another and even after a drop of one of the channels, its tone will still appear on the optical line because they were transferred to the rest of the channels that were not dropped. To avoid this problem, high frequency tones could be used (as they are too fast, the amplifiers cannot follow them) but it would lead to a cost increase (as narrowband electronics are less expensive) and a loss in sensitivity (again, if detection bandwidth is narrow the sensitivity increases) [18].

Other techniques commonly used for troubleshooting network faults are OSNR monitoring. Normally, the techniques capable of measuring signal power can also be utilized to obtain the optical noise power, which is extrapolated from the power level adjacent to the channel. However, there are some cases where that noise does not result only from the adjacent channel such as multi-path interference effects, amplifier pump laser relative intensity noise (RIN) transfer and FWM [18]. Consequently the use of these techniques in dense WDM networks or in presence of OADM (optical add-drop multiplexer) and OXC (optical cross-connect) is not effective [22]. In dense WDM networks there is little spectrum available for monitoring. The problem of using OADMs or OXCs is that different optical noise powers can be detected in adjacent channels (Figure 2.16).

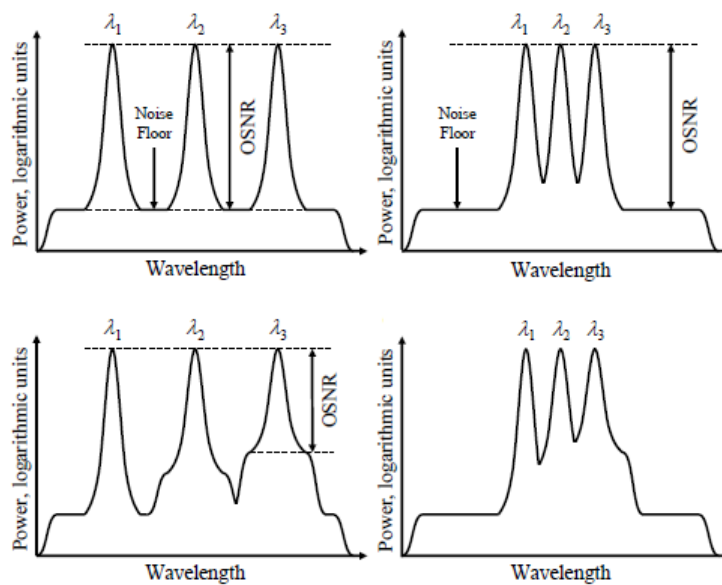


Figure 2.16. Limitations of OSNR monitoring technique in WDM network (top left), dense WDM network (top right), meshed WDM network (bottom left) and meshed dense WDM network (bottom right) [6].

The success of these type of monitoring depends greatly on the filters and modulation formats used that are specific for each system and reliable results demand a channel spacing of at least 100 GHz for 10 Gb/s signals [18]. Despite the inherent limitations, OSNR monitoring has proved to be an excellent measure of optical amplifier performance which is a frequent source of signal degradation.

There are others that are based on the measurement of the noise power present in a single channel bandwidth. This is a difficult task because the noise and the signal can be confused due to the random nature of the data signal, which can be incorrectly interpreted as noise [18]. A potential way to avoid this problem is using the optical polarization so the signal will have a well-defined polarization, unlike optical noise that will be unpolarized [23], like shown in Figure 2.17. This approach could be a solution but the polarization of an optical signal can change due to propagation and, although it is possible to compensate PMD, in ultra long-haul systems is almost impossible to track the polarization fluctuations [24].

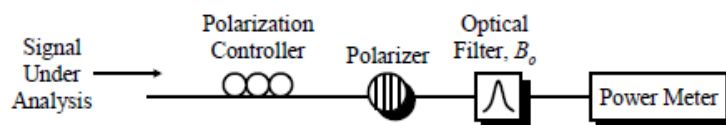


Figure 2.17. In-band OSNR system by Rasztovits-Wiech, 1998 [6].

OSNR monitoring has proven to be effective on localizing the existent faults, but cannot determine the root that caused the impairment, which is highly desirable in order to repair the network and reestablish the system normal operation. With the increase in bit rate, potentially harmful effects, such as CD and PMD, can degrade the signal so the monitoring of the accumulation of those effects may be needed to insure a good network management. Despite the existence of dispersive fibers or even other components that can compensate CD and PMD, there will always be some issues like malfunctions in those components or improper installation of some element. Besides that, if we consider a reconfigurable network the problem is even bigger, as dispersion becomes time dependent. If we want to know not only where the impairment is located but also which component was the fault origin, the use of a dispersion monitor alongside with noise monitoring is highly recommended [18].

CD is one of the impairments that can limit an optical network. Although, its linear behavior makes it relatively easy to compensate and minimize. Its compensation and monitoring are essential and several techniques were developed to monitor CD so the system can be properly compensated. Some methods demand changes in

transmitter and are applicable to WDM systems. One option is to detect the conversion of a PM signal into an IM signal due to CD [25]. Other approach requires the insertion of a subcarrier that measures its sidebands delay relative to the baseband [21].

There are also techniques that do not demand any change at the transmitter. One of those techniques [26] works by extracting the clock frequency from the data and monitor its RF power. This technique is useful as it is sensitive to many distortion effects, including PMD, which can help on fault localization. However, it cannot isolate chromatic dispersion and has the disadvantage of depending on bit rate and modulation format [26].

One good example of a powerful technique is the detection of the relative delay between the upper and lower vestigial-sideband (VSB) signals transmitted. Figure 2.18 shows how this technique can be implemented.

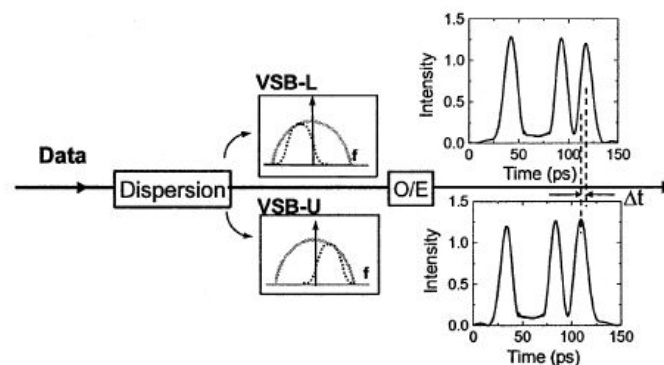


Figure 2.18. Vestigial-sideband technique [6].

Tuning an optical filter away from the optical spectrum center of the double-sideband data gives the lower and upper VSBs signals. Once they are at different wavelength ranges it will result in a relative group delay between both signals due to CD. Clock recovery and phase detection are needed to measure the phase delay. A big advantage of this technique is its high sensitivity and it is unaffected by PMD, fiber nonlinearities and transmitter chirp [6].

Another impairment that needs to be monitored is Polarization Mode Dispersion. PMD is the effect caused by the propagation at different velocities of the two orthogonal states of polarization of a single spectral component. One technique capable of measuring the differential group delay (DGD, i.e. instantaneous first-order PMD) is based in an RF tone where the optical frequency component is split on two principal states of polarization (PSPs). Each replica propagates with different velocities that dephase these replicas, reducing the spectral component in the RF power spectrum. It occurs because the dephasing results in destructive interference. DGD is measured the S-parameters of several spectral slices that were filtered from the baseband signal [27]. Figure 2.19 shows this technique procedure.

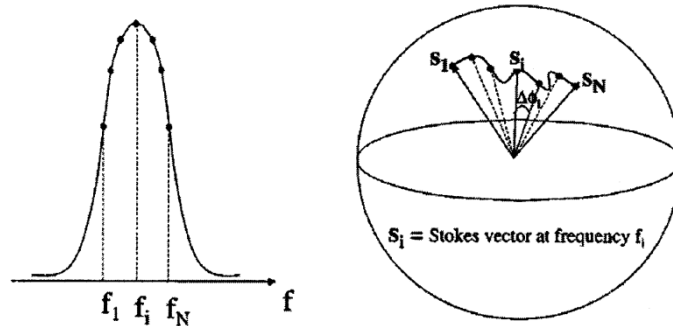


Figure 2.19. PMD monitoring: frequency sweep over the pulse spectrum (left) and S-parameters (right) [18].

Other approach is measure the phase difference between two optical frequency components for both PSPs. This technique, based on measuring the degree of polarization (DOP), does not depend on other possible degrading effects and do not demand high-speed circuits. However, it has several disadvantages. NRZ modulated signals suffer from lack of sensitivity on PMD detection and for RZ modulated signals the monitoring of DGD has small range [28]. Furthermore, this technique is affected by higher-order PMD [18].

Fault management usually opts on measuring BER or Q-factor and the best methods make use of asynchronous histograms. It can be made either in optical or electrical domain, as shown in Figure 2.20.

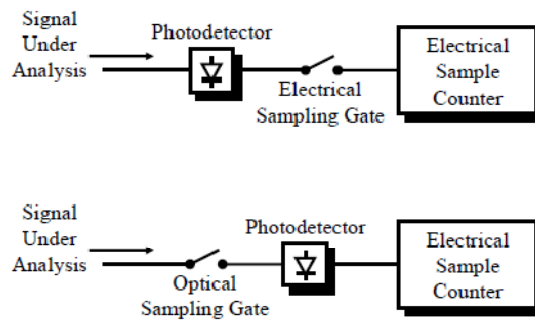


Figure 2.20. Histograms based on electrical sampling (top) and based on optical sampling (bottom) [6].

These techniques can monitor signals at different bit rates because it does not request any clock recovery system and another advantage is that it can use low sampling frequencies. In electrical sampling a fast photodetector is needed so the signal is detected with the less distortion possible. In optical sampling the photodetector bandwidth must be at least the same as the sampling frequency, which the value is intended to be the highest possible to avoid averaging effects [18].

Q-factor monitoring is made by recording the errors. It is done through changing the decision threshold voltage of the receiver, and keeping it distant from optimum level. Once the errors are recorded, a rate can be generated and it is possible to monitor any modification that may occur. Figure 2.21 shows the waveform and the power distribution of a signal with (Figure 2.21, bottom) and without amplified spontaneous emission (ASE) noise (Figure 2.21, top).

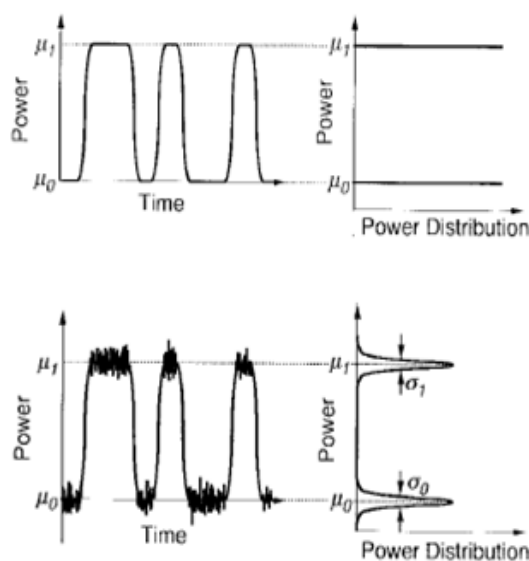


Figure 2.21. Waveform and power distribution of signal without ASE noise (top) and with ASE noise (bottom) [29].

Assuming that the distribution of ASE noise approximates Gaussian random variables and considering $\sigma_{1,0}$ and $\mu_{1,0}$ as standard deviation and mean value, respectively, of the marks/spaces rail of the output voltage, the Q-factor and the BER can be given by Equation 2.12 and 2.13 [29]:

$$Q = \frac{|\mu_1 - \mu_0|}{\sigma_1 + \sigma_0} \quad (2.12)$$

$$BER = \frac{1}{2} \operatorname{erfc}(Q/\sqrt{2}) \quad (2.13)$$

where $\operatorname{erfc}(x)$ is the error function.

Q-factor is, actually, BER. If Q-factor is measured using a receiver, it is electronic SNR. If it is measured by other means, like optical sampling, then it is in-band optical SNR. However, Q-factor monitoring usually demands clock recovery which can be undesirable if different bit rates are used [18]. To prevent these problem asynchronous histograms can be employed, as they record the amplitude histogram without any regard to timing [30].

Finally, timing jitter is also a problem and it is usually transmitter responsibility. Monitoring and compensation of such impairment is not easy and BER or Q-factor techniques can be utilized to determine the source of jitter [18].

Chapter 3. System Setup

In order to study this monitoring technique, a great number of simulations were performed using software program VPI [31]. The desired system was implemented and some parameters were tested to confirm the results. The scenario used as reference for the proposed technique aims to simulate a WDM optical network. It consists in N WDM channels, externally modulated, transmitting simultaneously with a CW probe signal through a standard single-mode fiber (SSMF). At the fiber end, the probe signal is filtered and analyzed (Figure 3.1).

As it was already referred, the purpose of this technique is to enhance the monitor of fiber nonlinearities, with special focus on XPM. XPM induces a phase shift on the probe resulting in frequency chirp. The phase variations are converted into power fluctuations as consequence of GVD presence. However, and once we are considering a WDM system, it cannot be ignored possible FWM effects that may interfere in the simulation results.

For a better understanding, the system will be divided in three main groups: emitter, fiber and receiver. Figure 3.1 shows the default system used.

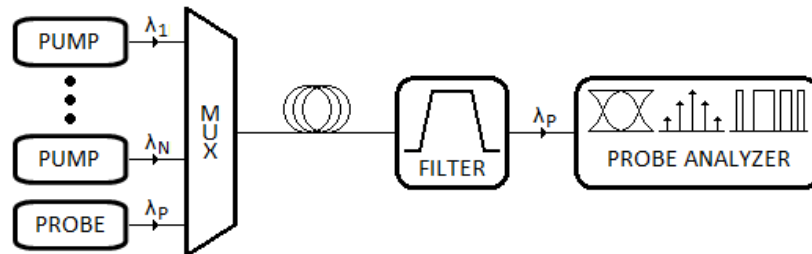


Figure 3.1. System Setup.

The following sections are sorted according to groups, where Section 3.1 relates to emitter, Section 3.2 is devoted to transmission and final Section 3.3 is about the receiver. Section 3.4 shows how the measurements are done.

3.1. Emitter

Emission group is divided in channels (externally modulated lasers transmitting random data) and probe (continuous wave laser in which we want to observe the XPM effects). The two are merged with an ideal multiplexer before propagating through a SSMF.

The goal is to study the behavior of the probe signal in a WDM system with a maximum of 16 channels operating in C-band. As so, simulations were made by setting some parameters and varying others, as one can see in Table 3.1.

The same happens in the probe signal transmitted alongside with the channel(s), where some parameters were changed and some were not, as it shows the Table 3.2.

<u>CONSTANT PARAMETERS</u>	
1 st Channel Emission Frequency	193,3 THz (1550,92 nm)
Laser Linewidth	0 Hz
Bit Stream Produced	Pseudo-Random Bit Sequence (PRBS)
Mark Probability of Ones	0,5 (50%)
<u>ADJUSTABLE PARAMETERS</u>	
Number of Channels	1 – 16
Bit Rate	2,5 or 10 Gb/s
Channel Spacing	50 or 100 GHz
Laser Average Power	10 or 32 mW (10 or 15 dBm)

Table 3.1. Channels parameters.

<u>CONSTANT PARAMETERS</u>	
Laser Linewidth	10 MHz
Laser Emission Frequency	193,45 THz (1549,72 nm)
<u>ADJUSTABLE PARAMETERS</u>	
Laser Average Power	0,1 or 1 mW (-10 or 0 dBm)

Table 3.2. Probe parameters.

An ideal multiplexer is used to combine all signals (channels and probe) before propagate in the fiber.

3.2. Fiber

A standard single-mode fiber was used and the most important parameters can be seen in the upcoming Table 3.3.

<u>CONSTANT PARAMETERS</u>	
Attenuation	0,2 e-3 dB/m
Dispersion Slope	0,08 e3 s/m ³
Nonlinear Index	2,6 e-20 m ² /W
Core Area	80 e-12 m ²
<u>ADJUSTABLE PARAMETERS</u>	
Fiber Length	10 – 50 km
Fiber Dispersion	6 – 26 ps/(nm.km)

Table 3.3. Fiber parameters.

3.3. Receiver

A rectangular band pass optical filter was used, before the analyzer, with a bandwidth of 4 * bit rate, and with a stop band of 90 dB.

The analyzer shows the optical spectrum, the waveform and the eye diagram of any channel. Waveform was mostly checked because the aim was to observe the variations suffered by the probe. Although, optical spectrum needed also some attention as the increasing of the number of channels causes new FWM components that must be considered. The variables monitored were taken from the VPI analyzer

[31] and are frequency chirp variance and intensity variance. They were both measured through its waveforms and calculated as shown in (3.1)

$$\sigma^2 = \frac{\sum(x-\bar{x})^2}{(n-1)} \quad (3.1)$$

where σ^2 is the variance, n is the sample size and \bar{x} is the sample mean. The variables were monitored under several system conditions since we intend to evaluate how XPM effects are influenced by some parameters adjustments.

3.4. Measurements

It was previously referred the interest of measure the frequency chirp variance and the intensity variance. To understand the principle of this technique, Figure 3.2 shows the intensity and frequency chirp waveforms before and after the propagation, considering 16 channels NRZ modulated (plus the probe), with a channel spacing of 100 GHz, at a bit rate of 10 Gb/s. Moreover, the channel power is 10 dBm, probe power is -10 dBm and the fiber has 50 km and its dispersion is 16 ps/(nm.km).

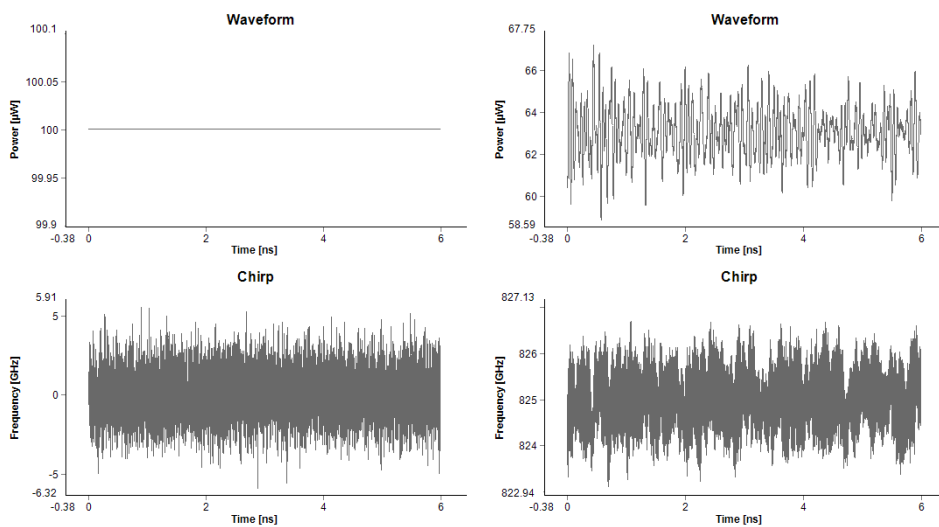


Figure 3.2. Intensity and frequency chirp waveforms before (left) and after (right) the propagation.

As one can see from the previous figure, probe signal gains an oscillatory structure after the propagation because of XPM. By measuring intensity and frequency chirp variances it is expected that those values could help to identify some of the systems' parameters and monitor the impact of the XPM.

Chapter 4. Simulation Results

As it was already explained, this simple technique makes use of a probe to monitor XPM. The aim is to know how the change of some of the WDM network parameters will affect the system, more specifically, the consequences that those alterations will produce in a probe signal through XPM, its chirp frequency and intensity variance fluctuations. Some parameters as fiber length and dispersion, channel and probe power, number of channels, modulation format, channel spacing and bit rate (see Tables 3.1 – 3.3) will be varied. Some of these variations will result in reducing or growing of XPM effects in the probe signal and that information may be vital in order to do the necessary adjustments to keep the network working properly. Besides, the behavior of the intensity and frequency chirp variances may be useful to identify and monitor some of the system's parameters. The following sections are divided according to each parameter variation.

Important Notes: Unless otherwise is said, the default parameters are:

- Probe Power: -10 dBm
- Number of Channels: 16
- Channel Power: 10 dBm
- Channel Modulation Format: NRZ
- Channel Spacing: 100 GHz
- Fiber Dispersion: 16 ps/(nm.km)
- Fiber Length: 50 km
- Bit Rate: 10 Gb/s

4.1. Fiber Length

The relation of fiber length with XPM is easily understandable. Long fibers will result in accumulation of XPM effects and, consequently, the degradation of the transmission. Unless it is prevented the overlap of the channels carrying simultaneously “1” bits, XPM effects will continue to deteriorate the network. Even though, Figures 4.1 and 4.2 show that frequency chirp variance is almost the same for all fiber lengths used. Once the optical fiber acts as a *bandpass filter*, the high-frequency components of the input signal are attenuated by the fiber. So, after the frequency chirp reaches its maximum value, it will begin to appear like an average. Introducing relative time delays among the channels could be a solution. By reducing the times that “1” bits of neighboring channels may overlap, XPM effects tend to be lower. Other possibility is using RZ format because “1” bits are shorter and return to zero before the bit duration is over. However it may not be a practical solution for high number of channels because, although “1” bits are shorter, if the average power of the

channel is the same for RZ and NRZ, it will result in twice of the power for “1” bits in RZ format (when considering RZ50, i.e. return-to-zero with 50% of duty-cycle), which leads to higher XPM effects.

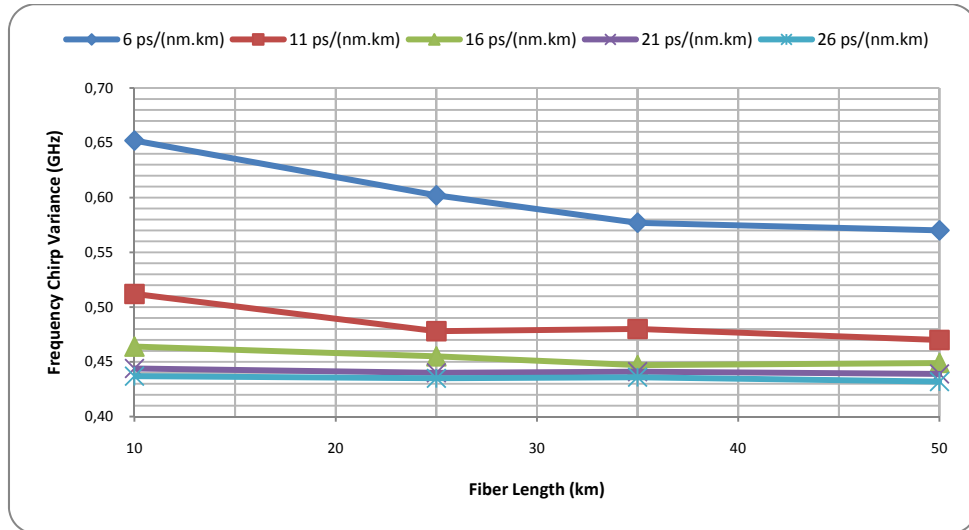


Figure 4.1. Frequency chirp variance vs. fiber length for different fiber dispersions.

Figure 4.1 shows frequency chirp variance in function of fiber length for different fiber dispersions for 16 channels and Figure 4.2 for different numbers of channels.

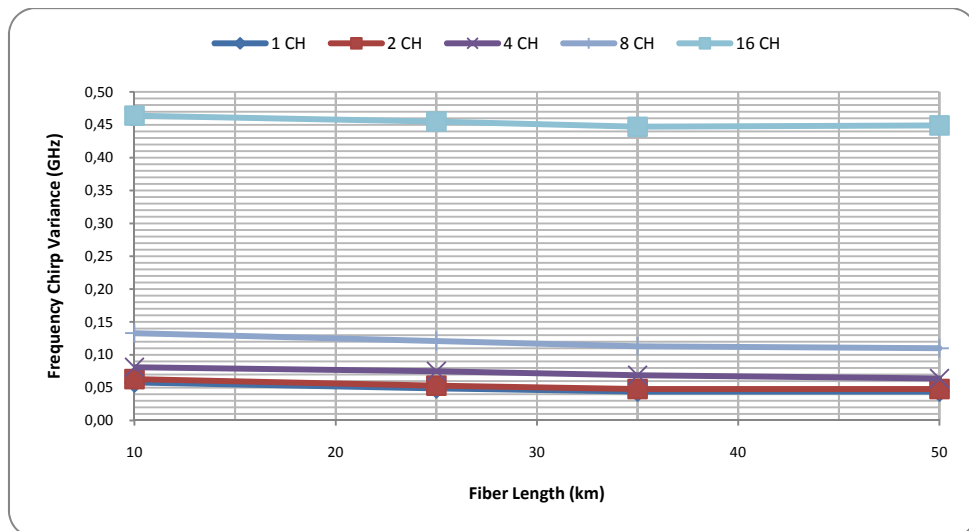


Figure 4.2. Frequency chirp variance vs. fiber length for different number of channels.

Alternatively to the usage of frequency chirp variance, another approach was taken. Although, it may not represent only XPM effects but can also consider other

impairments such as FWM. Measuring the intensity variance on the probe does not assure that we are monitoring only XPM as other phenomenons may modify the signal amplitude wave. Nevertheless, FWM was minimised and small impact was suffered. For that, the probe signal was shifted a few gigahertz and was confirmed that FWM new frequencies did not coincide with the chosen frequency of the probe and so the presented values of either frequency chirp and intensity variances are reliable.

Figure 4.3 show the dependence of intensity variance with fiber length for different fiber dispersions and it is easy to understand why intensity variance decrease with the distance. Because the variance is one measure of statistical fluctuations, averaging the squared distance of its possible values from the expected value (mean) (Equation 3.1), it is obvious that, once fiber becomes longer, the probe signal loses strength (the same happens with all channels) and its mean power value decreases. Identical process occurs with probe fluctuations that also decrease and, as consequence, lower values of variance are measured (once the number of samples is the same).

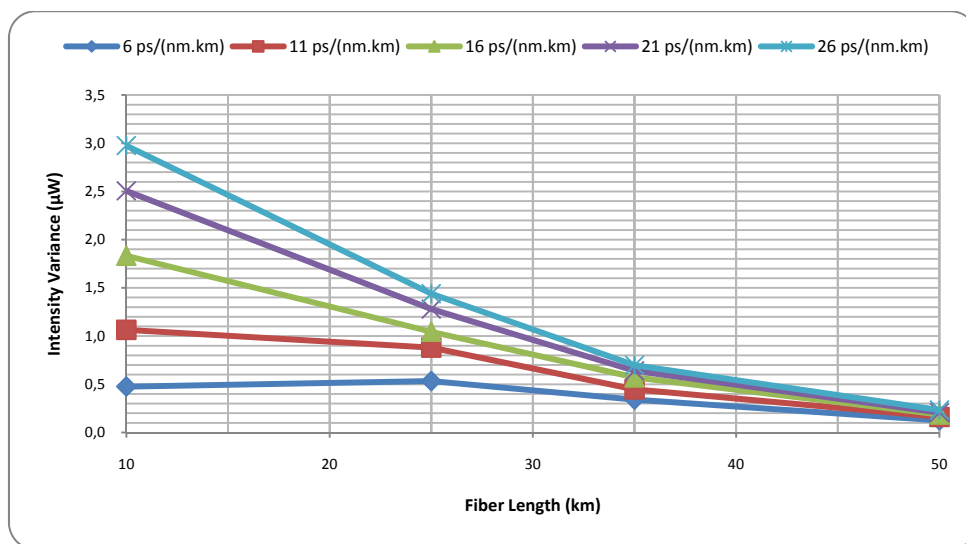


Figure 4.3. Intensity variance vs. fiber dispersions for different fiber lengths.

For fiber dispersions lower than 11 ps/(nm.km), intensity variance still increases after 10 km. After reaching the highest value, the intensity variance begins to decrease, just as in higher fiber dispersions. This issue will be discussed in the next section.

In conclusion, it is possible to monitor fiber length with this simple technique for different number of channels transmitting, maintaining parameters as channel power and probe power. The only exception is the case referred in the previous paragraph.

4.2. Fiber Dispersion

In Section 4.1 it was concluded that lower fiber dispersions resulted in particular behaviors in the first 20 km of fiber. For fiber dispersions lower than 11 ps/(nm.km), Figure 4.1 showed frequency chirp variance still decreasing after 10 km and Figure 4.4 shows intensity variance reaching its highest value also after 10 km (although it cannot be seen in the graphic because the measures were only done for 10, 25, 35 and 50 km, the peak is, for example, near 17,5 km for a fiber dispersion of 6 ps/(nm.km) and near 15 km for 11 ps/(nm.km), as shown in Figures 4.5 and 4.6, respectively).

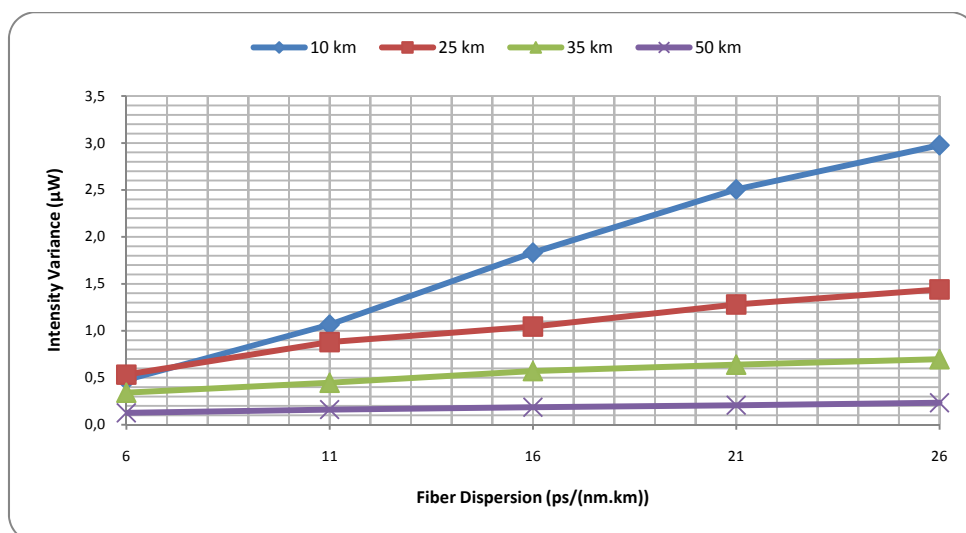


Figure 4.4. Intensity variance vs. fiber length for different fiber dispersions.

When pulses propagate inside optical fibers either dispersive or nonlinear effects may dominate, depending on initial pulse width (T_0) and its peak power (P_0).

Consider dispersion length (L_D) and nonlinear length (L_{NL}) as scales over which each effect become important, and given by Equations (4.1) and (4.2) [1]

$$L_D = \frac{T_0^2}{|\beta_2|} \quad (4.1)$$

$$L_{NL} = \frac{1}{\gamma P_0} \quad (4.2)$$

where β_2 is the GVD parameter and γ is the nonlinear parameter defined by Equation (2.7). The evolution of the pulses can differ depending on L_D and L_{NL} relation with the fiber length (L). When L is much smaller when compared with both L_D and L_{NL} , neither dispersive nor nonlinear effects are relevant during pulse propagation. However, when L_D or L_{NL} are similar to L , the correspondent effect must be considered (or even both at same time). So, Figures 4.1 and 4.4 show that dispersion is still accumulating after the first 10 km for lower fiber dispersions, while for values above 16 ps/(nm.km) dispersion is accumulated before.

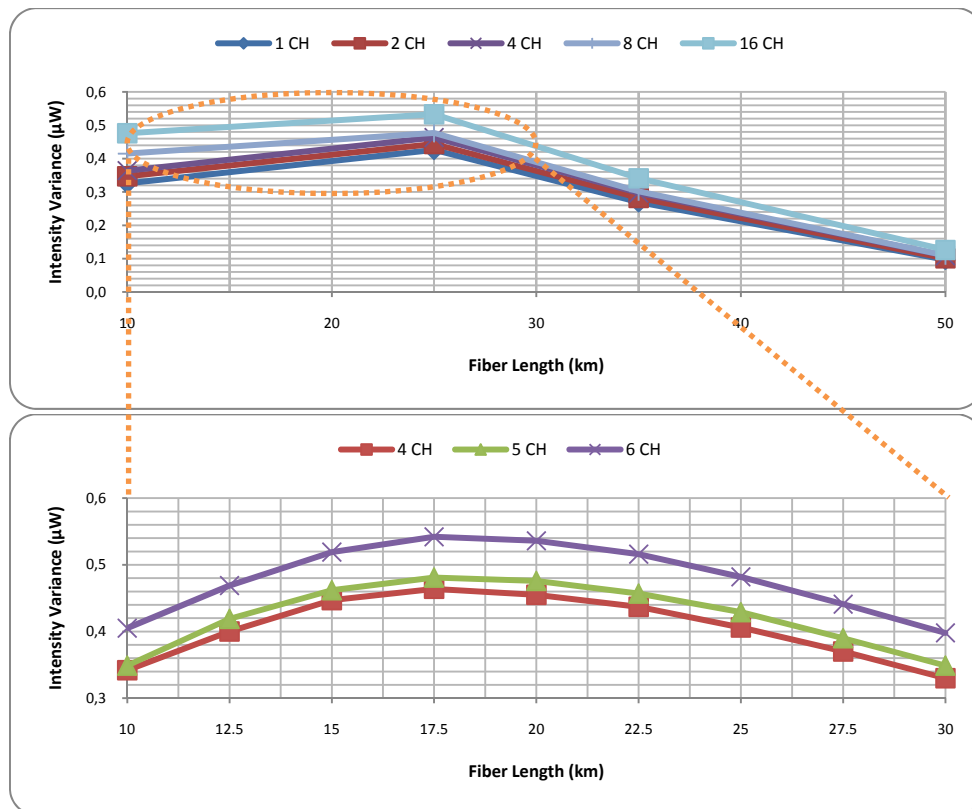


Figure 4.5. Intensity variance vs. fiber length for 6 ps/(nm.km) (top) and zoom at the region of the highest value of intensity (bottom).

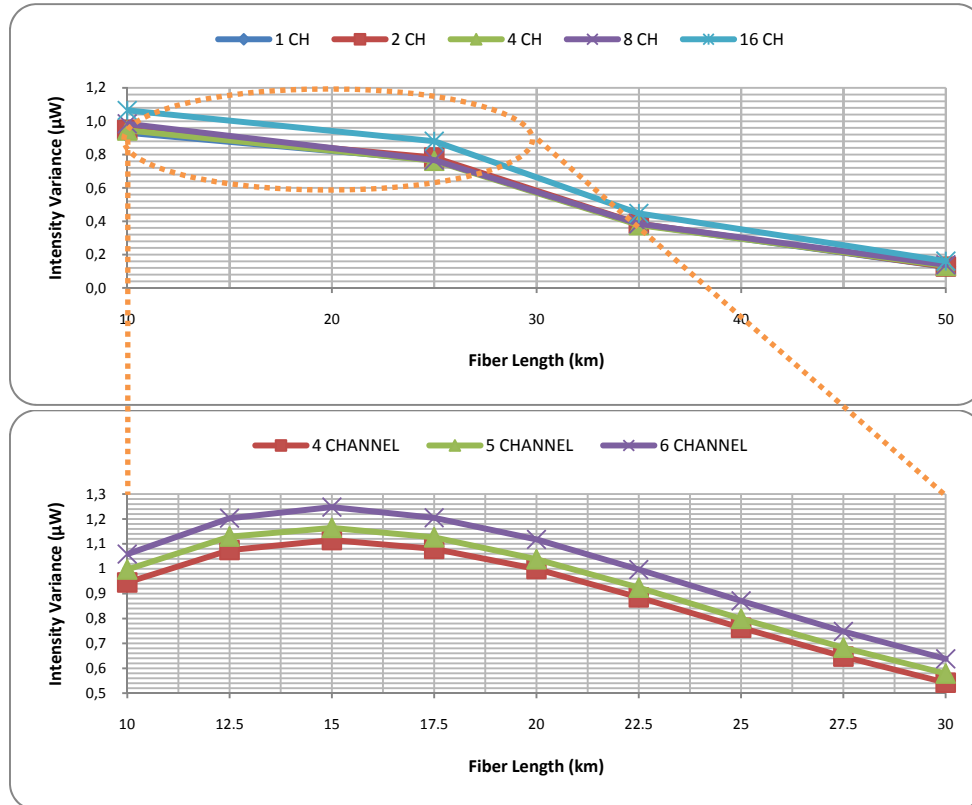


Figure 4.6. Intensity variance vs. fiber length for 11 ps/(nm.km) (top) and zoom at the region of the highest value of intensity (bottom).

Besides, one can see also from Figure 4.1 that frequency chirp variance greatly decreases with the increase of fiber dispersion value, in opposition with intensity variance that increases with fiber dispersion (Figure 4.4). When fiber dispersion increases, the walk-off distance becomes smaller and the interaction between the pulses decrease. This leads to lower values of frequency chirp variance. However, higher values of fiber dispersion result in higher PM-IM conversion, which explains the greater values of intensity variance when increasing dispersion.

In order to apply this technique to monitor fiber dispersion, two different ranges of values must be separated: under 16 ps/(nm.km) and above 16 ps/(nm.km). For the former group, the analysis of the frequency chirp variance is enough to identify different values of fiber dispersion. Contrarily, for the latter group, different values of fiber dispersion present almost the same frequency chirp variance. In this case, the information given by intensity variance could be a solution to monitor fiber dispersion as its values are easily distinguishable, when considering short fibers. For longer ones, the intensity variance tends to be the same, making the usage of this method rather

difficult (Figure 4.4). The conclusions are true if channels and probe power are maintained.

4.3. Channel Power

In Chapter 2 we discuss, with particular interest, the nonlinear phase shift that a signal may suffer under certain circumstances. It was referred that the refractive index seen by an optical field inside an optical fiber depends on the intensity of the copropagating fields, besides its own field (Equation 2.9). Once in a pump-probe configuration a signal that is much weaker than the rest of the channels transmitted is used, we can conclude that the phase shift suffered by the probe rely, in greatest part, on the power of the channels. Thereby, if that power is increased, the nonlinear phase shift will also increase and XPM effects become stronger, which implies higher frequency chirp as shown in Figure 4.7.

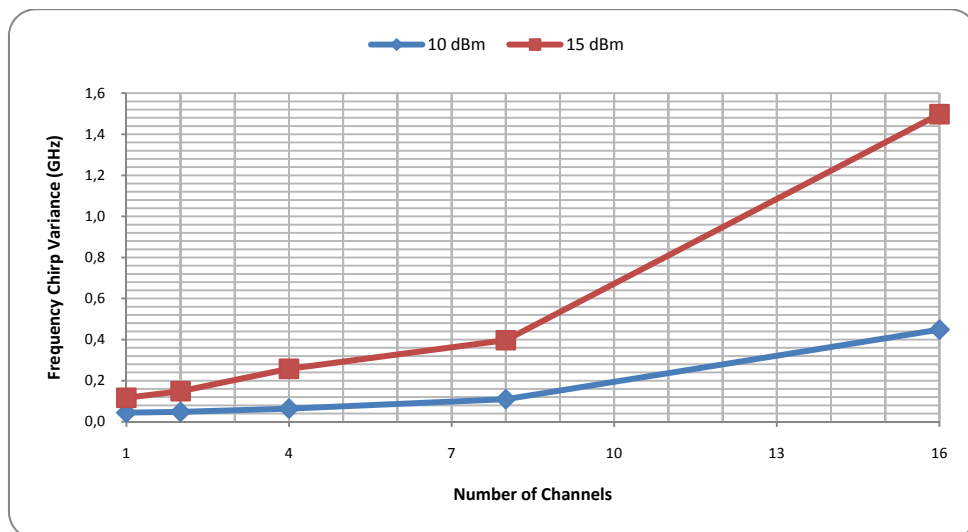


Figure 4.7. Frequency chirp variance vs. number of channels for different channel power.

It is also obvious that once nonlinear phase shift depends greatly on channels power, if such value is increased and considering the same GVD value, the intensity fluctuations suffered by the probe will also increase (Figure 4.8).

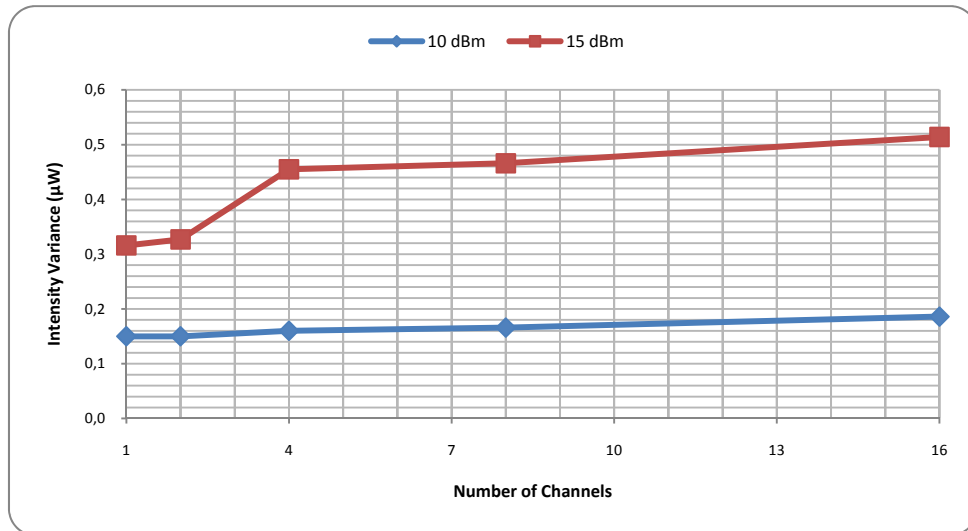


Figure 4.8. Intensity variance vs. number of channels for different channel power.

It is clear that, although XPM and other nonlinear effects are undesirable, they cannot be avoided. So, the efforts centralize on minimize the impairments that they create and, in what concerns with channel power, the problem can only be solved by reducing it. However, sometimes it is impossible to do it, since the signals must reach the receiver with enough power so they can be decoded. Therefore, it is extremely important to have knowledge of the power level needed by a signal at the end of the fiber to be properly received in order to create an optimization strategy that might be reducing the input power of the channels where the power received is beyond a certain value.

Figures 4.7 and 4.8 demonstrate that the analysis of either frequency chirp or intensity variance of the probe signal can be enough to monitor the power of the channels.

4.4. Probe Power

This technique is mainly based on a probe and it is through its analysis that conclusions are taken to give information to optimization and compensation systems.

Thus, it is essential to set the probe signal characteristics as good as possible so the information received is even more rigorous. One feature capable of adjustment is the power of the probe signal and Equation (2.10) shows that the probe nonlinear phase shift depend on its field and on copropagating fields. In previous section (4.3) it was mentioned that once probe was weak its field would not interfere on nonlinear phase shift. In this case, the simulations will focus on the consequences of increasing the probe power.

Until now it was only considered probe signal with -10 dBm. Figure 4.9 show that, if that power is increased, for example, to 0 dBm, the frequency chirp variance largely decreases when comparing to default case of -10 dBm. That it justified by the fact that probe field must be now considered and the copropagating fields do not have the same weight on nonlinear phase shift as before. So, the XPM effects on the probe are stronger when $P_{pump} \gg P_{probe}$ which explains the lower values for frequency chirp variance.

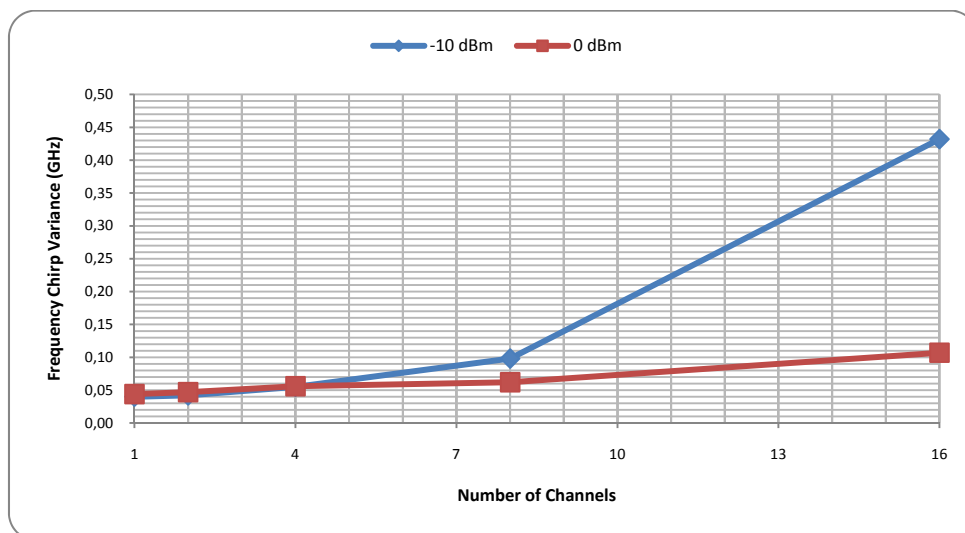


Figure 4.9. Frequency chirp variance vs. number of channels for different probe power.

Like the case of channels power, it is easy to understand that higher probe power values give rise to higher values of intensity variance once GVD is maintained and, consequently, nonlinear phase shift increases. Figure 4.10 shows that, when using probe power of -10 dBm, the intensity fluctuations are much smaller than for 0 dBm, like expected. Once variance depends on the mean value of a sample, the

intensity variation suffered by a probe with average power of 0 dBm is higher than for -10 dBm, even though its frequency chirp variance is lower.

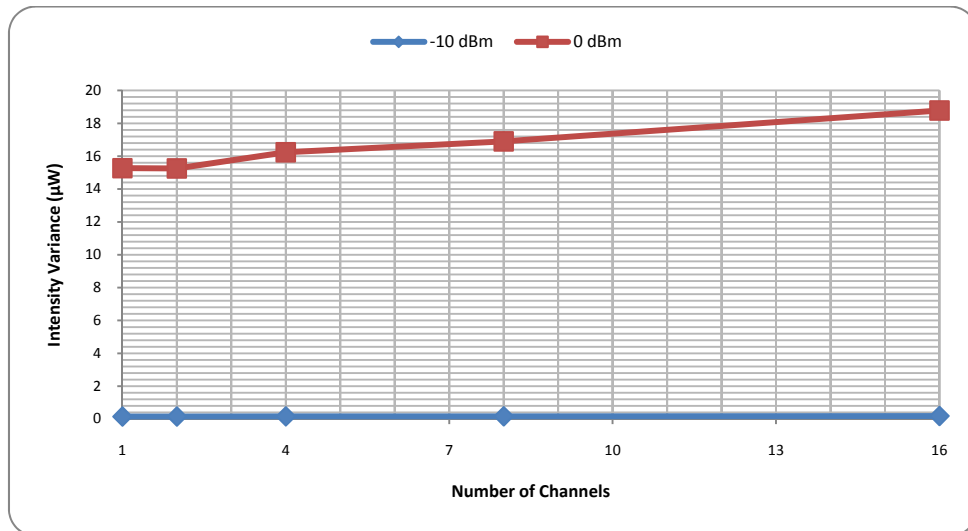


Figure 4.10. Intensity variance vs. number of channels for different probe power.

However, our intention is to measure the XPM effects with as much precision as we can, which means that probe power has to be low so it is possible to observe the fluctuations correctly. Although, one cannot forget that it has to be guaranteed the sufficient probe power at the receiver.

4.5. Number of Channels

The number of channels present in a WDM system have great impact on nonlinear effects. One of the aims of next generation optical networks is to offer an huge bandwidth, distributed to as many users as possible, over the longest possible distance. However, the increasing number of channels leads to a serious degradation of the network performance, because nonlinearities as FWM and XPM contribute to signal impairment (like it was referred in Chapter 2). To solve this issue, an additional amount of power may be needed at the receiver to maintain BER the same as it was in the absence of those nonlinearities. Still, the extra power might give raise to further

damage as it has the potentiality to grow even more the XPM effects, as it was concluded in Section 4.3 analysis.

As the focus is on XPM effects, we assured once more that new frequencies generateb by FWM did not coincide with probe frequency and, therefore, the FWM effects can be considered negligible.

The nonlinear phase shift suffered by the probe signal depends non only on the square of the intensity of its field but also on the square of the intensity of the other copropagating fields. Once probe signal is much weaker than the rest of the channels, its power almost do not influentiate the phase shift. Hence, the graphics that relate the frequency chirp variance with the number of channels transmitting behave like an 2nd order polynomial. That behavior maintains, even when changing system paramenteres such as fiber length (Figure 4.11), fiber dispersion (Figure 4.12), channel average power (Figure 4.7) and probe power (Figure 4.9).

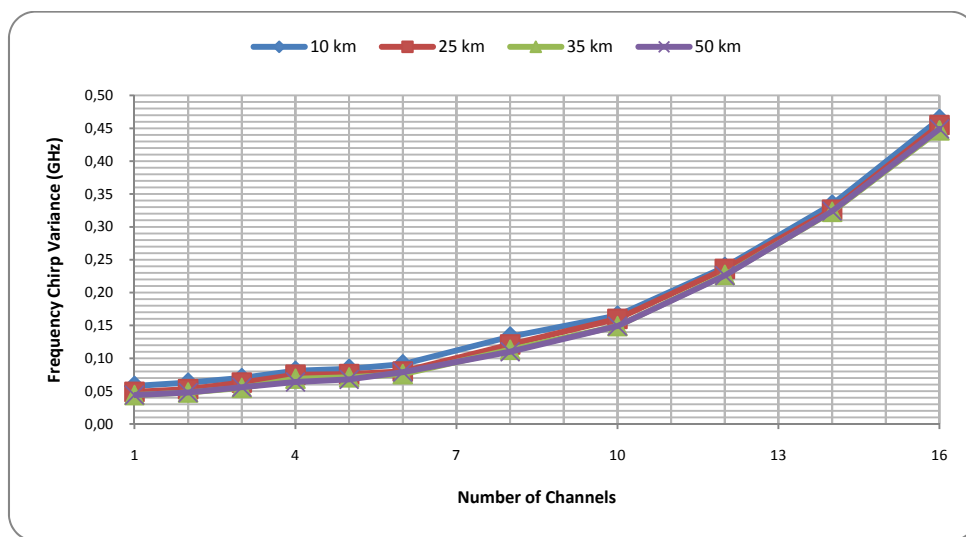


Figure 4.11. Frequency chirp variance vs. number of channels for different fiber length.

As it was discussed in Section 4.1, one can see from Figure 4.11 that frequency chirp variance is nearly the same for different fiber lengths, even when the number of channels increase. XPM effects for different fiber dispersion were also discussed previously, in Section 4.2, and Figure 4.12 confirms the polynomial behavior in that case too.

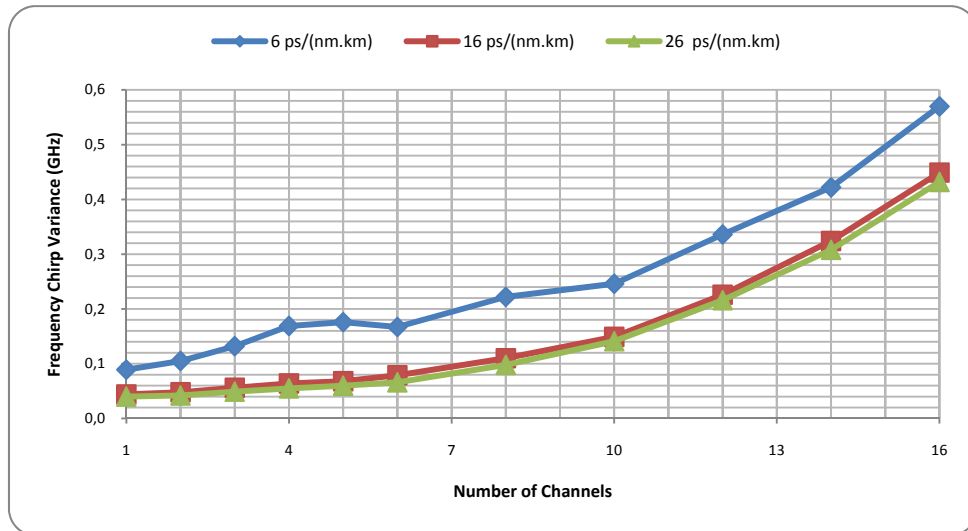


Figure 4.12. Frequency chirp variance vs. number of channels for different fiber dispersion.

One important information to retain from this is that this parameter is optimum for monitoring the number of channels in the propagation.

4.6. Modulation Format

In Chapter 2, two modulation formats were presented, NRZ and RZ, their advantages and disadvantages. The selection of each network modulation format is very important as different formats may behave differently, under the same conditions. This work only uses the simple cases of amplitude modulation, like NRZ and RZ (it was considered RZ with duty cycles of 33% and 66% which are referred as RZ33 and RZ66, respectively).

Once the same laser average power for NRZ and RZ was maintained, it is expected that, for a great number of channels, the intensity variance of RZ format will be higher. Although the “1” bits of RZ format are shorter (and, consequently, the walk-off distance is smaller), they have the same average power as the NRZ ones. As so, their interaction results in stronger XPM effects (that issue was discussed previously in

Channel Power Section). Figure 4.13 proves that point, although it was expected that the two types of RZ format should present different intensity variance values.

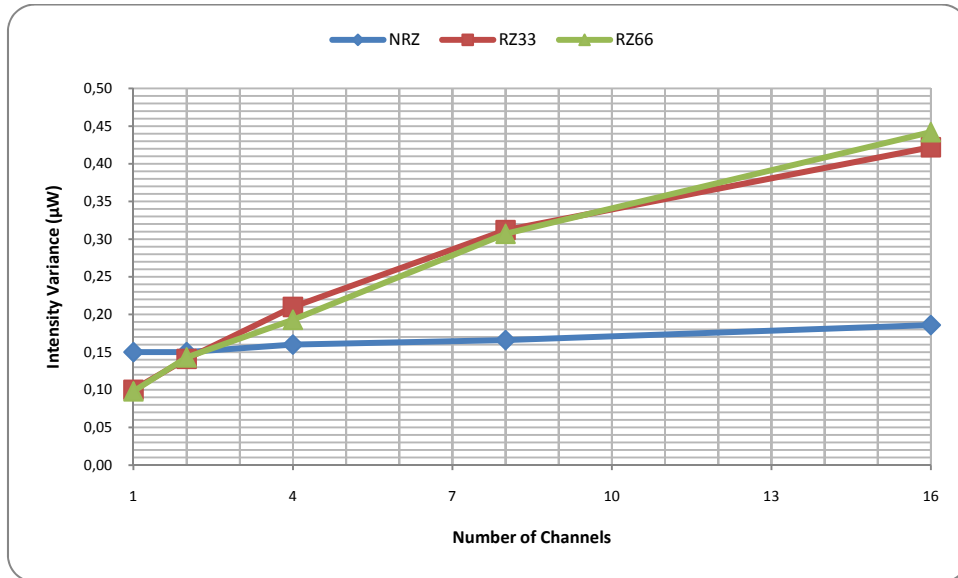


Figure 4.13. Intensity variance vs. number of channels for different modulation formats.

Figure 4.14 shows the frequency chirp variance for the three cases and the analysis of that measurement shows that RZ formats have higher frequency chirp variance than NRZ until the 10th channel. As the number of channels grow, frequency chirp variance of NRZ format begins to increase at a higher rate than RZ33 and RZ66, which increase almost at a constant rate.

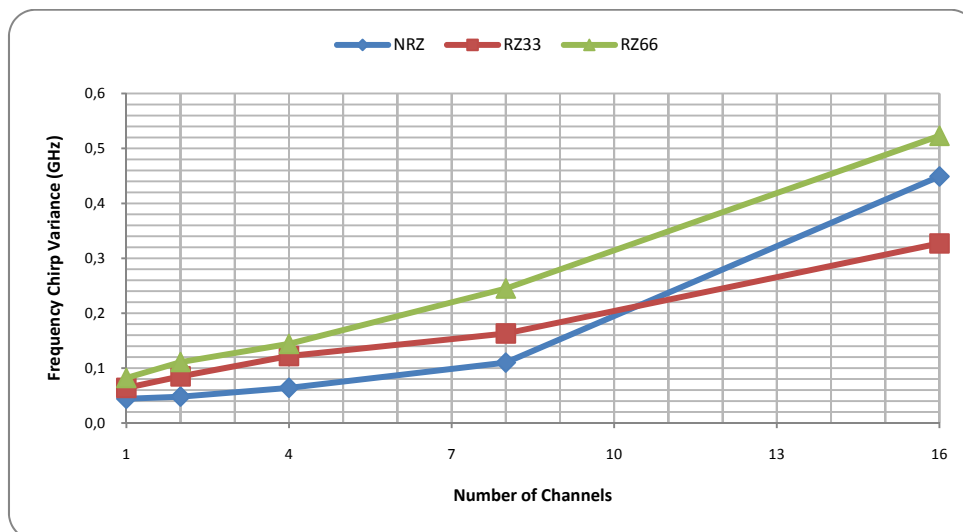


Figure 4.14. Frequency chirp variance vs. number of channels for different modulation formats.

It is difficult to identify the modulation format with this technique. However some conclusions can be reached. Intensity variance can tell which modulation type is used (NRZ or RZ), but it cannot monitor which is the duty cycle, in RZ case. Frequency chirp variance may be a complement on determining the duty cycle as it can be seen from Figure 4.14 in which RZ66 has a higher value than RZ33. These results are true if channel power, probe power, channel spacing and bit rate are input parameters.

4.7. Channel Spacing

In Chapter 1 it was mentioned that Fifth Generation networks aim to transmit even more channels by extending the window of operability or by decreasing the space between them. However, that ambition still faces some problems once the effects of impairments such as FWM and XPM become even more significant when reducing channel spacing. Until this point, all results were considering only channel spacing of 100 GHz. In this section it was reduced to 50 GHz and Figure 4.15 shows the comparison between both cases for intensity variance.

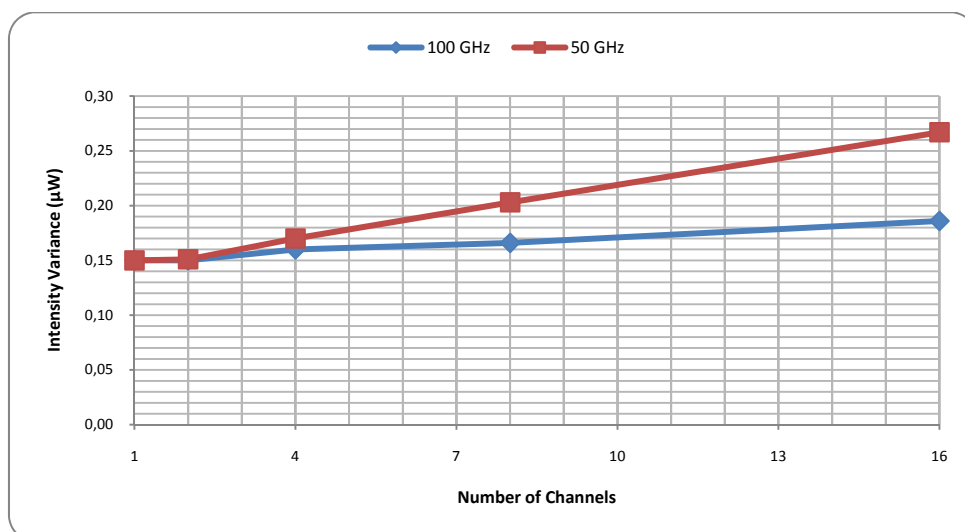


Figure 4.15. Intensity variance vs. number of channels for different channel spacing.

One can easily conclude from Figure 4.15 that narrow channel spacing induce higher values of intensity variance. The closer the channels are, the more is the time that pulses interact, i.e. the walk-off distance is longer. Consequently, XPM effects are stronger and intensity fluctuations of the probe signal increase.

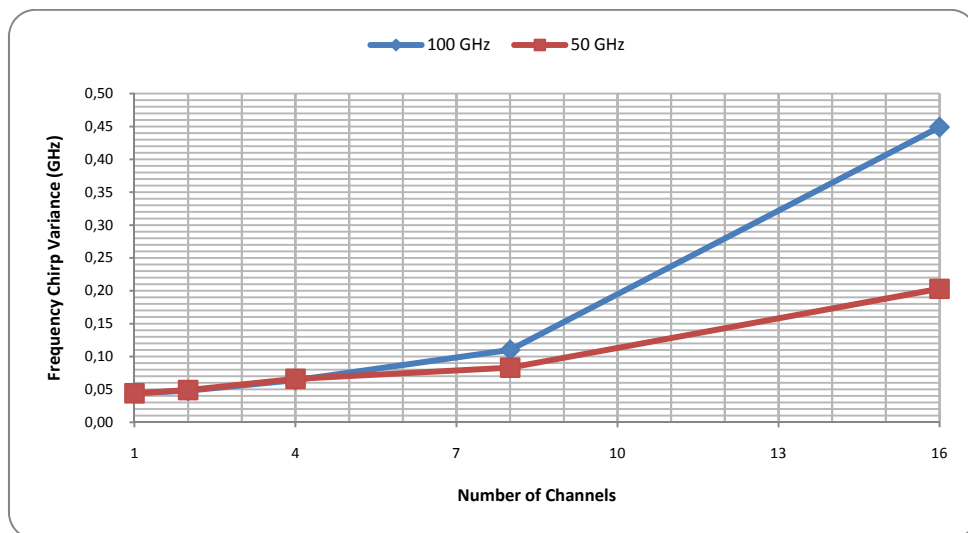


Figure 4.16. Frequency chirp variance vs. number of channels for different channel spacing.

Figure 4.16 shows that frequency chirp variance is higher for channels widely spaced, on contrary to what was expected. It was supposed that a channel spacing of 50 GHz would present a higher frequency chirp variance than for 100 GHz case, just like it occurred for intensity variance. Considering the same fiber dispersion and assuming that the intensity fluctuations depend on the PM-IM conversion, it is difficult to understand how lower values of frequency chirp variance (for channel spacing of 50 GHz) result in higher ones for intensity variance. It was thought that, because channel spacing was reduced to 50 GHz and the probe frequency was 193,45 THz, some of the new frequencies generated by FWM would coincide with the probe. If that was the case, the increasing of the intensity variance measurements would be logic. However, more simulations were done and it was confirmed that it was not that case. Despite this incoherency, the analysis of intensity variance proves to be trustful to monitor channel spacing. The measurements show the expected behavior, i.e., narrow channel spacing increases XPM degrading effects, if channel power, probe power and bit rate are maintained.

4.8. Bit Rate

In previous section it was discussed the consequences of decreasing the channel spacing because of the demand of the next generation networks on having more channels transmitting in a given bandwidth. As it was referred in this work Introduction, another major feature that new networks want to achieve is even higher bit rates than the ones already existing. However, this aspiration meets, once more, the nonlinearities problem because the increase of bit rate enhances XPM effects. Even though frequency chirp variance is slightly bigger for 10 Gb/s when compared to 2,5 Gb/s (Figure 4.17), the intensity distortions are much more significant when using higher speed systems (Figure 4.18).

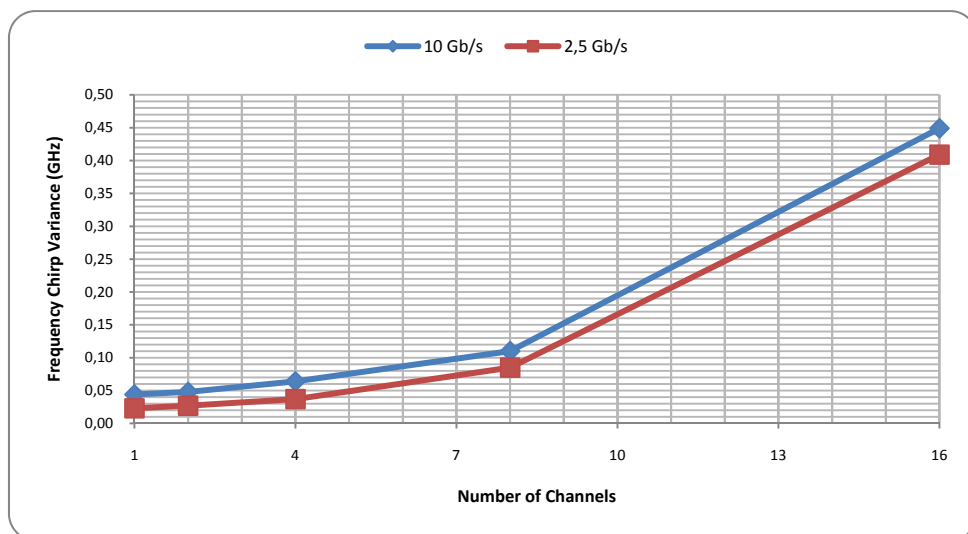


Figure 4.16. Frequency chirp variance vs. number of channels for different bit rate.

As Figure 4.18 shows, at higher bit rates the XPM distortion increases once there are more pulse transitions occurring in a given time interval. Using a bit rate of 10 Gb/s there is more PM-IM conversion, which results in much bigger value of intensity variance (when compared to 2,5 Gb/s). Frequency chirp is nearly the same (Figure 4.17) and, even though higher for 10 Gb/s, it was expected that the difference would be much bigger when comparing with the bit rate of 2,5 Gb/s.

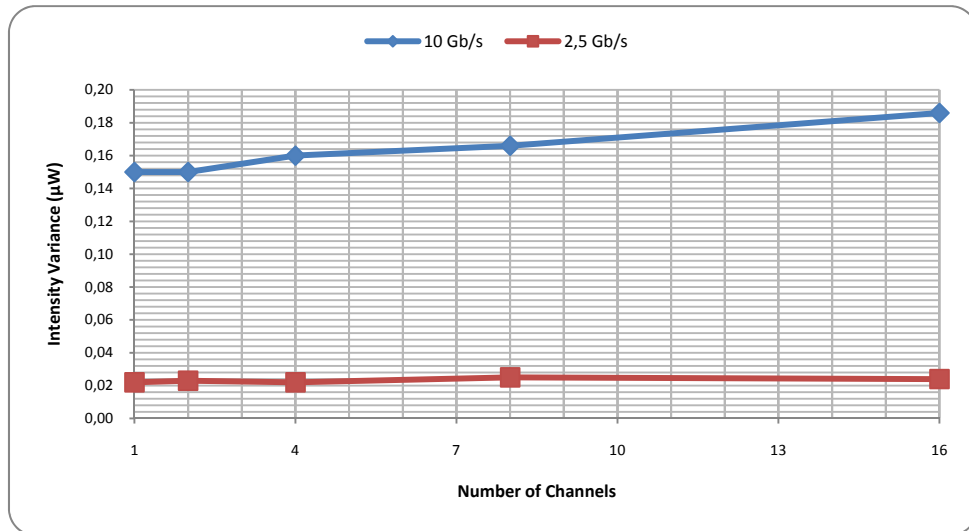


Figure 4.18. Intensity variance vs. number of channels for different bit rate.

Considering the two measurements, one can identify the system bit rate and that task is easier with the intensity variance values. If channel power, probe power and channel spacing are maintained, one can conclude that this simple technique is also capable of monitoring the bit rate.

Chapter 5. Final Conclusions

In previous section it was discussed the results of this work simulations. Each parameter was analyzed separately and some conclusions were made. In order to a better understanding of this technique efficiency, Table 5.1 presents a summary of all conclusions (FCV is Frequency Chirp Variance; IV is Intensity Variance; Both when the two measurments are needed simultaneously; if FCV and IV are marked is because thay can both monitor the given parameter). In Table 5.1 one can see which parameters can be monitorized with this work method and which measurments are needed for achieving that.

	<u>FCV</u>	<u>IV</u>	<u>Both</u>	<u>Input Parameters</u>
<u>Fiber Length</u>		✓		Ch. Power, Probe Power
<u>Fiber Disp.</u>			✓	Ch. Power, Probe Power
<u>Ch. Power</u>	✓	✓		Probe Power
<u>Num. Channels</u>	✓			
<u>Mod. Format</u>			✓	Ch. Power, Probe Power, Ch. Spacing, Bit Rate
<u>Ch. Spacing</u>		✓		Ch. Power, Probe Power, Bit Rate
<u>Bit Rate</u>	✓	✓		Ch. Power, Probe Power, Ch. Spacing

Table 5.1. Summary of the monitoring opportunities.

It is also important to recap some important notes regarding some studied parameters, and it can be seen in Table 5.2.

	<u>NOTES</u>
<u>Fiber Length</u>	Rather difficult to monitor fiber length when fiber dispersion is under 11 ps/(nm.km)
<u>Fiber Disp.</u>	FCV to monitor fiber dispersions under 16 ps/(nm.km); IV to monitor fiber dispersions above 16 for fiber lengths under 25 km (difficult for longer fibers)
<u>Mod. Format</u>	IV identifies modulation type (NRZ or RZ); FCV identifies RZ duty cycle (RZ33 or RZ66)
<u>Ch. Spacing</u>	Incomprehensive FCV results
<u>Bit Rate</u>	Easier to identify the bit rate with IV (although, still possible with FCV)

Table 5.2. Important notes regarding some parameters.

This technique showed some good monitoring opportunities for the studied parameters. However, some work still can be done and this method could be more useful if it could be applied to even more scenarios (like channels with different average power, channels with delays, etc.). In addition, this simple technique results are only based in computer simulations and thus some experimentals are needed to confirm its validity. Also, the analysis of the reflections in the fiber suffered by the monitoring channel would represent an opportunity for having all the monitoring physically co-located, however this requires further studies.

References

- [1] Govind P. Agrawal, *Nonlinear Fiber Optics*, Third Edition, Academic Press, 2001
- [2] J. Toulouse, "Optical Nonlinearities in Fibers: Review, Recent Examples, and Systems Applications", *Journal of Lightwave Technology*, vol. 23, no. 11, November 2005
- [3] Govind P. Agrawal, *Fiber-Optic Communications Systems*, Third Edition, John Wiley & Sons, 2002
- [4] L. F. Mollenauer, "Solitons in Optical Fibres and the Soliton Laser", *Royal Society, Discussion on New Developments in the Theory and Application of Solitons*, London, England, Nov. 1, 2, 1984
- [5] L. F. Mollenauer and R. H. Stolen "The Soliton Laser", *Optics Letters*, Vol. 9, Issue 1, pp. 13-15, 1984
- [6] Ruben Soares Luís, "Design and Optimization of Optical Routing Techniques and Devices", *Universidade de Aveiro*, DETI, 2007
- [7] S. P. Majumder, Redwan Noor Sajjad, Meer Nazmus Sakib and Nazmul Alam "Impact of Four Wave Mixing and Accumulated ASE on the Performance of a Metropolitan Optical Network", *ICON '06, 14th IEEE International Conference on Networks*, 2006
- [8] Jose A. Lazaro, Victor Polo, Carlos Bock, Mireia Omella and Josep Prat, "Remotely Amplified SARDANA: Single-fibre-tree Advanced Ring-based Dense Access Network Architecture", *32nd European Conference on Optical Communications (ECOC)*, 2006
- [9] Jianjun Yu, Zhensheng Jia, Philip N. Ji and Ting Wang, "40-Gb/s Wavelength-Division-Multiplexing Passive Optical Network with Centralized Lightwave Source", *Conference on Optical Fiber communication (OFC) / National Fiber Optic Engineers Conference (NFOEC)*, 2008

- [10] Toshio Morioka, "Ultrafast Optical Technologies for Large-Capacity TDM/WDM Photonic Networks", *Journal of Optical and Fiber Communications Research*, 2007
- [11] V. Bobrovs, J. Porins and G. Ivanovs, "Influence of Nonlinear Optical Effects on the NRZ and RZ Modulation Signals in WDM Systems", *Electronics and Electrical Engineering*. – Kaunas: Technologija, No. 4(76). – P. 55–58, 2007
- [12] Ron Hui, S. Zhang, B. Zhu, R. Huang, C. Allen and D. Demarest, "Advanced Optical Modulation Formats and Their Comparison in Fiber-Optic Systems", *Technical Report ITTC-FY2004-TR-15666-01*, January 2004
- [13] T. Minami, H. Nishimoto, M. Suyama, H. Kuwahara, T. Horimatsu and T. Touge, "Optical Amplification and Modulation Techniques for Multigigabit IM/DD Long-Haul Transmission Systems", *Fujitsu Laboratories*, 1990
- [14] Mônica de L. Rocha, Miriam R. X. de Barros, Maria F. de Oliveira, Mariza R. Horiuchi, Sandro M. Rossi, João B. Rosolem, Antonio A. Juriollo, Antonio C. Sachs and Alberto Paradisi, "Effects of External Modulation Transmission at 10 Gb/s Without Dispersion Compensation Through an All-Optical Node Concatenation", *Microwave and Optoelectronics Conference*, 2003
- [15] Charles H. Cox III, Gary E. Betts and Leonard M. Johnson, "An Analytic and Experimental Comparison of Direct and External Modulation in Analog Fiber-Optic Links", *Microwave Theory and Techniques*, vol. 38, no. 5, May 1990
- [16] L. Terlevich, S. Balsamo, S. Pensa, M. Pirola and G. Ghione, "Design and Characterization of a 10-Gb/s Dual-Drive Z-Cut Ti:LiNbO₃ Electrooptical Modulator", *Journal of Lightwave Technology*, vol. 24, no. 6, June 2006
- [17] Hsu-Feng Chou and John E. Bowers, "High-Speed OTDM and WDM Networks Using Traveling-Wave Electroabsorption Modulators", *IEEE Journal of Selected Topics in Quantum Electronics*, vol. 13, no. 1, January 2007

- [18] D. C. Kilper, R. Bach, D. J. Blumenthal, D. Einstein, T. Landolsi, L. Ostar, M. Preiss and A. E. Willner, "Optical Performance Monitoring", *Journal of Lightwave Technology*, vol. 22, no. 1, January 2004
- [19] T. Luo, C. Yu, Z. Pan, Y. Wang, J. E. McGeehan, M. Adler and A. E. Willner, "All-Optical Chromatic Dispersion Monitoring of a 40-Gb/s RZ Signal by Measuring the XPM-Generated Optical Tone Power in a Highly Nonlinear Fiber", *IEEE Photonics Technology Letters*, vol. 18, no. 2, January 15, 2006
- [20] K. J. Park, H. C. Ji and Y. C. Chung, "Optical Channel Monitoring Technique Using Phase-Modulated Pilot Tones", *IEEE Photonics Technology Letters*, vol. 17, no. 11, November 2005
- [21] G. Rossi, T. E. Dimmick and D. J. Blumenthal, "Optical Performance Monitoring in Reconfigurable WDM Optical Networks Using Subcarrier Multiplexing", *Journal of Lightwave Technology*, vol. 18, 2000
- [22] D. C. Kilper, S. Chandrasekhar, L. Buhl, A. Agrawal and D. Maywar, "Spectral monitoring of OSNR in high speed networks", in *28th European Conference on Optical Communication (ECOC)*, September 2002
- [23] M. Rasztoivits-Wiech, M. Danner and W. R. Leeb, "Optical Signal-to-Noise Ratio Measurement in WDM Networks Using Polarization Extinction", in *24th European Conference on Optical Communication (ECOC)*, 1998
- [24] B. C. Collings and L. Boivin, "Nonlinear Polarization Evolution Induced by Cross-Phase Modulation and its Impact on Transmission Systems", *Photonics Technology Letters*, IEEE, vol. 12, November 2000
- [25] A. Chraplyvy, R. Tkach, L. Buhl and R. Alferness, "Phase Modulation to Amplitude Modulation Conversion of CW Laser Light in Optical Fibers", *Electronic Letters*, vol. 22, April 1986

- [26] G. Ishikawa and H. Ooi, "Demonstration of Automatic Dispersion Equalization in 40 Gb/s OTDM Transmission", in *24th European Conference on Optical Communication (ECOC)*, 1998
- [27] G. Bosco, B. E. Olsson and D. J. Blumenthal, "Pulsewidth Distortion Monitoring in a 40 Gbit/s Optical System Affected by PMD", *Photonics Technology Letters*, IEEE, vol. 14, 2002
- [28] Nobuhiko Kikuchi, "Analysis of Signal Degree of Polarization Degradation Used as Control Signal for Optical Polarization Mode Dispersion Compensation", *Journal of Lightwave Technology*, vol. 19, no. 4, April 2001
- [29] Shoko Ohteru and Noboru Takachio, "Optical Signal Quality Monitor Using Direct Q-Factor Measurement", *IEEE Photonics Technology Letters*, vol. 11, no. 10, October 1999
- [30] J. D. Downie and D. J. Tebben, "Performance Monitoring of Optical Networks with Synchronous and Asynchronous Sampling", in *Optical Fiber Communication Conference (OFC)*, 2001
- [31] VPI Transmission Maker 8.0 (build 305), www.vpisystems.com